(T 4) TOYODA, H., *J. Phys. Soc. Japan* **14**, 376 (1959).
(T 5) TAUREL, L., DELAIN, C. and GUÉRIN, C., *Compt. rend.* **246**, 304 (1958).
(T 6) TOYODA, H., WAKU, S. and HIRABAYASHI, H., *J. Phys. Soc. Japan* **14**, 1003 (1959).
(T 7) TOYODA, H., *J. Phys. Soc. Japan* **15**, 1539 (1960).
(W 1) WIEDER, H. H., U. S. Naval... Ordnance Lab., Corona, Calif., Tech. Memo No. 42-6, September (1957).
(W 2) WOOD, E. A. and HOLDEN, A. N. *Acta Cryst.* **10**, 145 (1957).
(W 3) WIEDER, H. H., *J. Appl. Phys.* **30**, 1010 (1959).
(Z 1) KIYASU ZEN'ITI, HUSIMI, K. and KATAOKA, K. *J. Phys. Soc. Japan* **13**, 661 (1958).

CHAPTER III

POTASSIUM DIHYDROGEN PHOSPHATE AND ISOMORPHOUS CRYSTALS

1. Introduction

Potassium di-hydrogen phosphate, KH_2PO_4, often referred to in abbreviated form as KDP, crystallizes in the tetragonal system at room temperature. This phase belongs to the non-centrosymmetrical point group $\bar{4}2m$; therefore, it is piezoelectric. A transition occurs at 123 °K into a ferroelectric phase with orthorhombic symmetry and point group *mm*. The polar axis lies along the direction of the *c* axis of the tetragonal phase. The ferroelectric activity was first reported by Busch and Scherrer (B 1) in 1935, and since then a very large number of papers have been published on the subject of the physical properties of this crystal.

A number of isomorphous compounds, obtained by substitution of potassium by rubidium or cesium, and phosphorous by arsenic, have also been found to undergo ferroelectric transitions at low temperatures. These compounds are discussed in Section 6 of this Chapter. Substitution of potassium by ammonium leads to the isomorphous ammonium di-hydrogen phosphate, $NH_4H_2PO_4$ (abbreviated ADP) which undergoes a transition to an antipolar state at -125 °C, the antipolar direction being parallel to one of the *a* axis of the room-temperature tetragonal phase.

Large, colorless single crystals of KDP can be grown easily from water solutions, mainly by slow evaporation of a saturated solution at constant temperature. A detailed study of the conditions under which very large, clear crystals can be grown was carried out by Walker (W 1) for the case of ADP and the results are useful in part for the case of KDP. The crystals are prismatic, elongated along the [001] axis, with large (100) and (101) faces.

2. Dielectric Properties and Non-linearity

The dielectric constant measured along the *a* axis (ε_a), and that along the *c* axis (ε_c), are both of the order of 50 at room temperature. Upon cooling, ε_c increases hyperbolically and reaches a very high value, of the order of 10^5, at the transition temperature T_c (see Fig. III-1). Below this temperature, ε_c drops quite sharply, but not discontinuously. This drop can be explained on the basis of the dielectric saturation effects observed above the Curie point (see Section II-3), since the dielectric constant decreases when the crystal is polarized with an external d.c. field. In the ferroelectric region, the polarization is spontaneous and causes a decrease of ε_c with increasing polarization.

The component ε_a also shows an anomaly at the transition temperature, although much less pronounced than that exhibited by ε_c. This is an indication that the dielectric co-operative phenomenon also affects the component along the tetragonal a axis.

In a temperature range of about 50 ° C above the transition temperature, the dielectric constant ε_c follows the Curie–Weiss law: $\varepsilon_c \cong C/(T - T_0)$ with $C = 3250$ ° and $T_0 = -150$ °C (B 3). Thus, the Curie–Weiss temperature T_0 coincides with the transition temperature T_c.

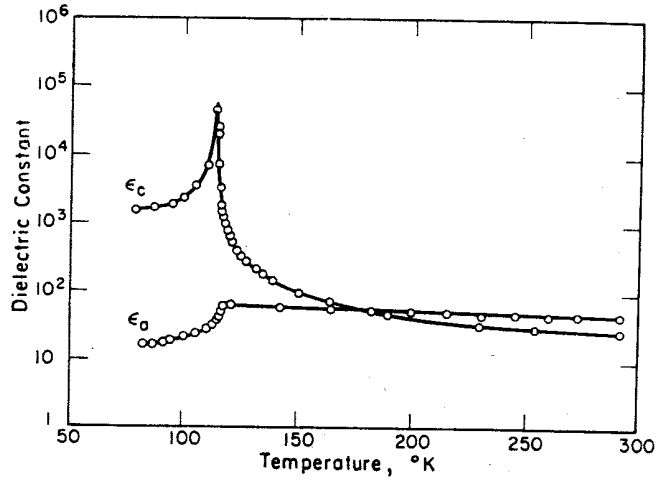

FIG. III-1. Dielectric constant of KH_2PO_4 as a function of temperature (according to Busch (B 2)).

The Curie–Weiss law is obeyed for measuring field frequencies up to the order of 10^7 c/s (B 3). No relaxation of the dielectric constant ε_c is found, except for the dispersion due to piezoelectric resonance, up to frequencies of the order of 10^{10} c/s (M 1). The measurement of the dielectric constant with a low-amplitude a.c. field of very high-frequency yields information about the dielectric behavior of the clamped crystal. At frequencies that are above the piezoelectric dispersion, mechanical resonance is suppressed and the crystal is clamped by inertia. It should be noted, however, that below the Curie temperature, the crystal is only partially clamped because the spontaneous polarization cannot be suppressed with this technique. Therefore, the application of high-frequency fields does not affect the Curie temperature. In order to "clamp" the spontaneous polarization we should suppress the spontaneous strain. This is impossible to achieve in practice because, as we already know, the crystals split into domains, each of which keeps its spontaneous strain although the crystal as a whole has zero strain. Nevertheless, Baumgartner's measurements of the clamped crystal (B 3), using frequencies of 10^7 c/s, yield two important results, viz:

(i) The Curie–Weiss temperature of the clamped crystal lies about 4 °C lower than that of the free crystal, thus indicating that the effect of total clamping would reduce the Curie temperature by this amount.

(ii) The fact that the Curie–Weiss law is unaffected by the use of high frequencies, i. e. the Curie constants of the clamped and the free crystal are the same, indicates that the difference between the reciprocal susceptibilities of the clamped and the free crystal is essentially temperature independent. We can express this difference in terms of the constants introduced in the fundamental equations of a piezoelectric crystal as defined in Section I-5. In fact, from Eqs. (I-4a), (I-4b), (I-5a), (I-5b) we obtain

$$\chi^x = \chi^X + ab = \chi^X(1 + ad), \tag{III-1}$$

and we conclude, therefore, from the experimental data that the product of the pertinent constants ab, or $\chi^X ad$, is temperature independent.

Baumgartner also performed very extensive measurements of the dependence of the dielectric constant ε_c upon field and polarization in a narrow temperature region above the transition temperature (B 4). These were the first measurements of this kind ever carried out on ferroelectric crystals and the experimental techniques used were the following. The field dependence of the dielectric constant was investigated by applying a large d.c. biasing field upon the crystal; as we have seen in Section II-5, this technique yields the value of the adiabatic dielectric constant for zero stress as a function of the field (and, of course, the temperature). The polarization dependence of the dielectric constant was investigated by first measuring the polarization as a function of the field with a ballistic galvanometer, then differentiating the results to obtain the isothermal dielectric constant as a function of polarization (and temperature). Comparison of the two sets of data yields the difference between isothermal and adiabatic values of the dielectric constant, which is discussed in detail in Section II-5. This difference is quite large in the vicinity of the transition point, because KDP shows a very marked electrocaloric effect; about 1 °C above the transition temperature, a field of 10^4 V/cm causes an adiabatic temperature change of more than 1 °C. The experimental results can be written in terms of the adiabatic dielectric susceptibility in the following way:

$$\frac{1}{k_S} = \frac{4\pi}{C}(T - T_0) + A''_H(P, O) + \frac{16\pi^2}{C^2}\frac{T}{c_P}P^2, \tag{III-2}$$

and the similarity between this expression and Eq. (II-9a) is quite obvious. Thus, the correction terms consist of two contributions, viz. a saturation term and an adiabatic term. The *saturation* term $A''_H(P, O)$ is the second derivative of the higher order terms of the free energy function with respect to polarization. Unfortunately, the coefficients of the terms with higher orders of P in the free energy expansion are not known for KDP, but they could be computed from Baumgartner's data. It appears that the contribution of the sixth and higher power term in the free energy expansion cannot be neglected. The *adiabatic* term,

$$\frac{16\pi^2}{C^2}\frac{T}{c_P}P^2,$$

can be computed as soon as the specific heat at constant polarization, c_P, is known. Baumgartner's data yield $c_P = 0.977$ J/cm³ °C.

The two correction terms of the dielectric constant are plotted as functions of polarization in Fig. III-2. It is seen that, for polarization values lower than about 2×10^{-6} C/cm², the adiabatic term is larger than the saturation correction, but the situation is reversed at higher polarizations.

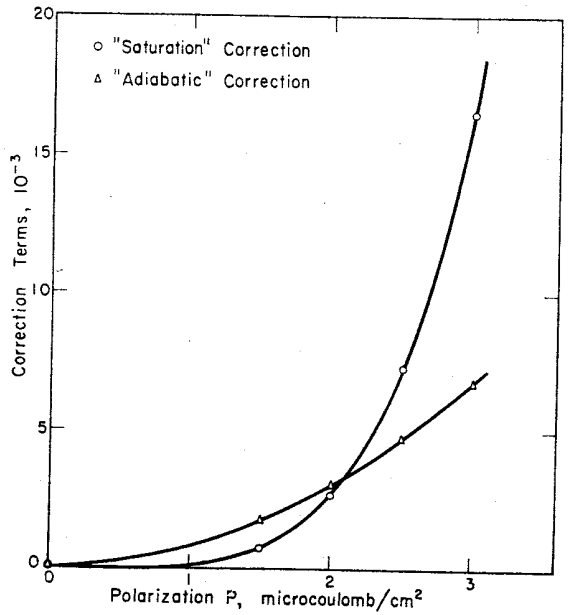

FIG. III-2. Saturation and adiabatic correction terms of the dielectric constant of KDP, as computed from Baumgartner's measurements (B 4) by Devonshire (D 1).

The field dependence of the dielectric constant ε_c is depicted in Fig. III-3, which is a logarithmic plot of ε_c vs. the reduced temperature $(T - T_c)$ for different values of the d.c. biasing field. This is a different representation of the behavior depicted in Fig. II-8 for tri-glycine sulfate. It should be noted that the effect of an electric field is to blur the transition, so that we can no longer speak of a transition in the usual sense (D 1). However, we see that the peak of the dielectric constant is displaced toward higher temperatures by the biasing field.

The temperature dependence of the spontaneous polarization P_s is shown in Fig. III-4. At 100 °K, i.e. 23° below the transition point, $P_s = 4.7 \times 10^{-6}$ C/cm². Two qualitative observations can be made on the behavior of the spontaneous polarization of KDP, viz:

(i) the onset of P_s at the transition point occurs continuously, the transition is of the second order; yet,

(ii) the rise of P_s at the transition temperature is quite rapid, as compared for example to that shown by tri-glycine sulfate. Qualitative comparison with

Eq. (II-2) would seem to indicate that, for KDP, the coefficient ξ is small and the coefficient ζ is more relevant (K 4).

The low-frequency coercive field E_c is of the order of 2 kV/cm at approximately 100 °K and apparently shows marked fluctuations from sample to sample. It is interesting that at approximately 60 °K a sharp break is observed in the tempera-

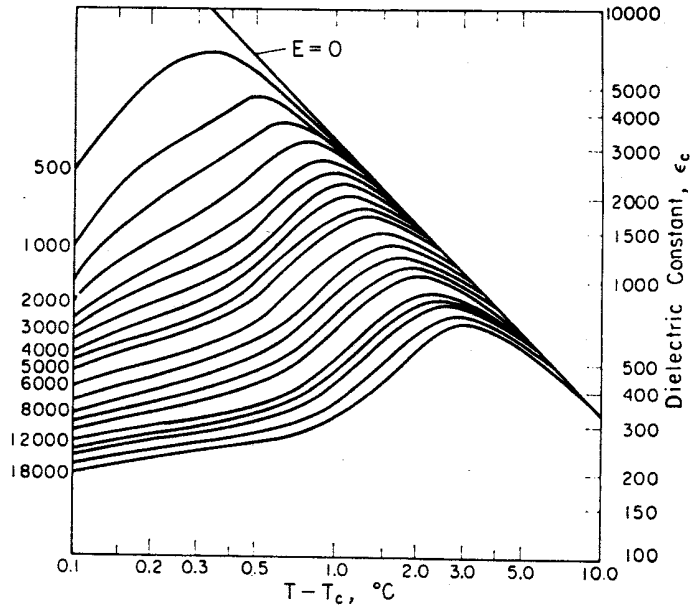

FIG. III-3. Dielectric constant ε_c of KDP as a function of reduced temperature $(T - T_c)$ for different values of the d.c. biasing field E. The E values are given for each curve on the left hand side (according to Baumgartner (B 4)).

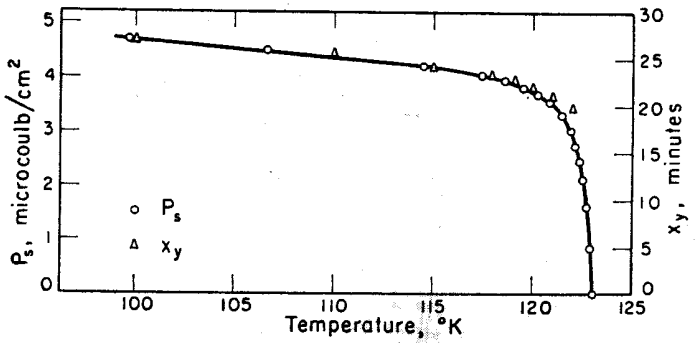

FIG. III-4. Spontaneous polarization of KDP as a function of temperature (according to von Arx and Bantle (V 1)). The triangles represent measurements of the spontaneous shear and are referred to the ordinate axis on the right (according to de Quervain (D 2)).

ture dependence of E_c, and this quantity increases rapidly at lower temperatures (Fig. III-5). This is probably due to hindered domain-wall motions at these temperatures.

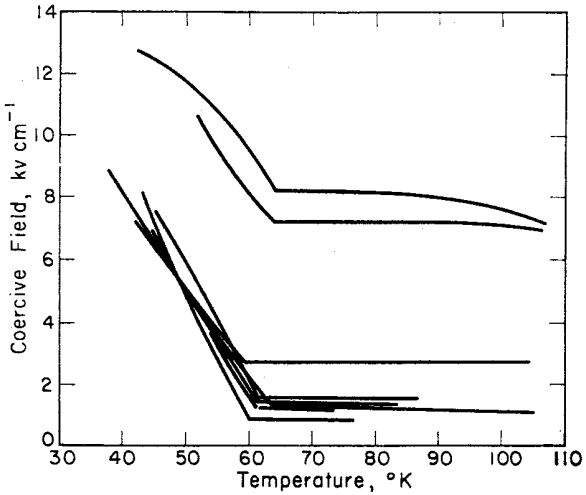

FIG. III-5. Coercive field E_c of different samples of KDP as a function of temperature (according to Barkla and Finlayson (B 5)).

3. Specific Heat and Lattice Distortion

The Specific Heat

The specific heat of KDP was measured by a number of authors. Considerable discrepancies are found both in the details of the shape of the specific heat curve and in the value of the transition heat obtained by integration. Figure III-6 shows the temperature dependence of the specific heat at constant pressure as measured by Stephenson and Hooley (S 1). At the transition point, an anomaly with the typical λ-shape is observed. The transition energies of KH_2PO_4 and the isomorphous compounds KD_2PO_4 and KH_2ASO_4 are listed in Table III-1.

It should be pointed out, in connection with the typical λ-shape of the specific heat anomaly, that the thermodynamic relation (II-5)

$$\Delta c_p = \frac{2\pi}{C} T \frac{\partial P^2}{\partial T},$$

is verified satisfactorily by the experimental data (V 2) for KDP.

The Lattice Distortion

The linear expansion coefficients of KDP were measured by de Quervain (D 2), as functions of temperature, with X-ray methods. The volume expansion coefficient $(1/V)(dV/dT)$ was computed to be equal to 8.2×10^{-5}. The relative variation

of the lattice sp[illegible]ngs with temperature is depicted in Fig. III-7. In order to understand the structural distortion that occurs spontaneously at the transition temperature, we first need to clarify the coordinate system to which we refer. Crystal morphology and other crystallographic considerations favor the choice

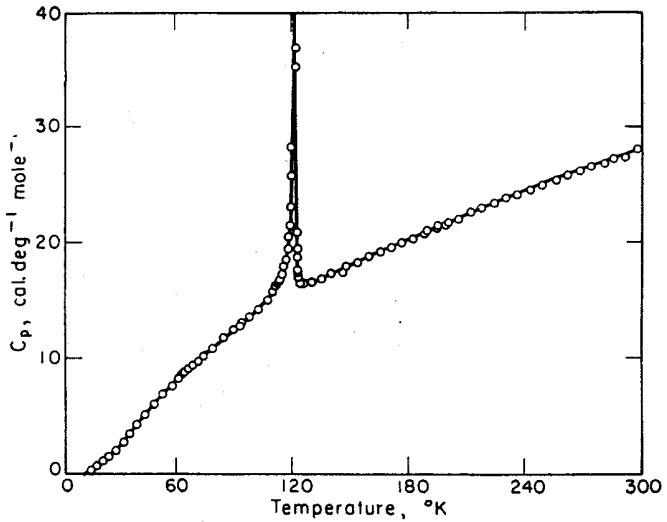

FIG. III-6. Specific heat of KDP as a function of temperature (according to Stephenson and Hooley (S 1)).

TABLE III-1. TRANSITION ENERGIES OF KH_2PO_4, KD_2PO_4 AND KH_2AsO_4

Substance	Curie temperature (°K)	Heat of transition ΔQ (cal/mole)	Transition entropy ΔS (cal/mole °C)	References
KH_2PO_4	123	57	0.47	BANTLE (B 6)
		87	0.74	STEPHENSON and HOOLEY (S 1)
		87	0.74	DANNER and PEPINSKY (D 3)
KD_2PO_4	213	100	0.47	BANTLE (B 6)
KH_2AsO_4	97	84	0.87	BANTLE (B 6)
		84	0.90	STEPHENSON and ZETTLEMOYER (S 6)

of a reference system in which the a_1 and a_2 axes are perpendicular to the major faces of the crystal. The corresponding unit cell has a square cross-section with $a_1 = a_2 = 7.453$ Å. Figure III-8(a) shows schematically this cross-section and the lattice distortion which occurs at the transition temperature, the c axis being perpendicular to the plane of the figure. The spontaneous strain consists of a slight change in length of a_1 and a shear $x_{12} = x_6 = x_y$, which amounts to 27′ at approximately 20° below the transition temperature (D 2). It would appear

logical to describe the distorted cell in terms of pseudo-monoclinic axes a_1 forming an angle of $90° + x_y$ with each other. However, the true symmetry of the low-temperature phase is orthorhombic, and the unit cell has a rectangular cross-

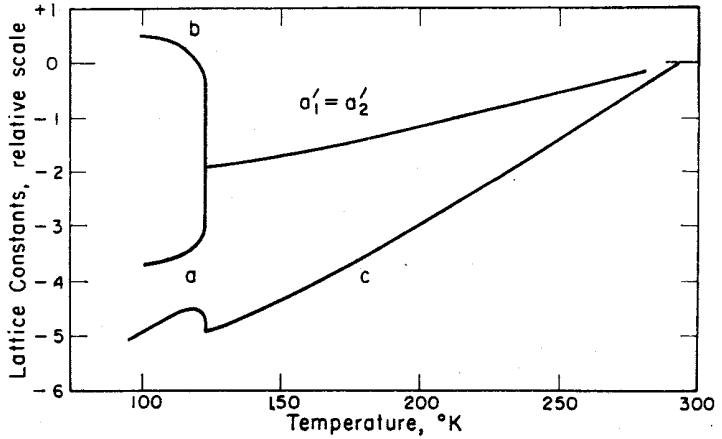

FIG. III-7. Temperature dependence of the lattice constants of KDP. The ordinate scale represents the deviation from the room temperature values in units of 10^{-2} Å (according to de Quervain (D 2)).

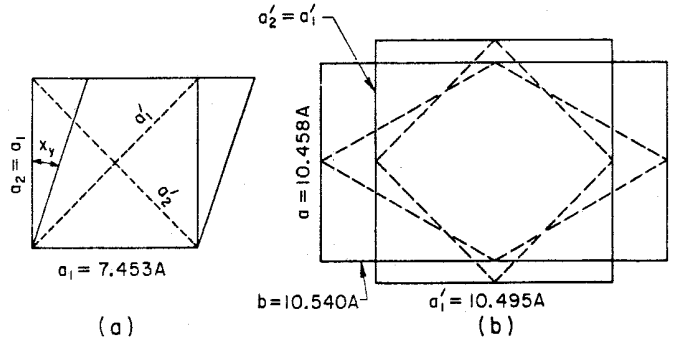

FIG. III-8. Unit cells and lattice distortion in KDP (schematic). (a) The lattice distortion consists of a slight change in a_1 and a shear x_y, (b) The lattice distortion is an elongation of $\mathbf{a}_1'$ to a and a compression of a_2' to b.

section approximately along the directions a_1', a_2' of the original [110] axes. With this in mind, it may be more convenient, for certain purposes, to adopt the larger tetragonal cell (with edges $a_1' = \sqrt{(2)}a_1$) from the beginning. Then the spontaneous strain consists in a slight elongation of the a_1' axis (which becomes the orthorhombic b axis) and a simultaneous contraction of the a_2' axis (orthorhombic a axis) (Fig. III-8b). It is the relative behavior of the $a_1' = a_2'$ and the c axes, which is shown in Fig. III-7. The relation between the orthorhombic parameters a, b and

the monoclinic parameters a_1, $(90° + x_y)$ is the following:

$$a = 2a_1 \cos \frac{90° + x_y}{2},$$

$$b = 2a_1 \sin \frac{90° + x_y}{2}.$$

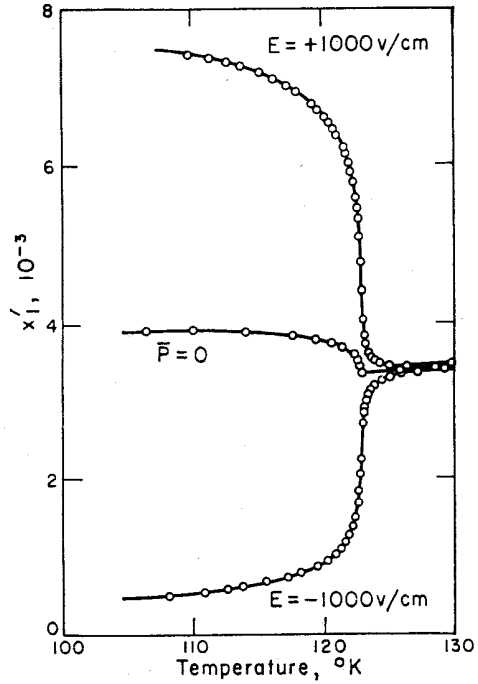

FIG. III-9. Elongation of a_1' and contraction of a_2' in KDP measured interferometrically in the vicinity of the transition temperature (according to von Arx and Bantle (V 1)).

The lattice distortion was also measured by von Arx and Bantle (V 1) using Fizeau's interference method to determine the elongation of a_1' and the contraction of a_2' at the transition temperature. Figure III-9 shows the result of these measurements. A d.c. field of 1000 V/cm was applied in order to polarize the crystal uniformly along the c direction. The *mean value* of the two curves also shows an anomaly at 123 °K, indicating that the expansion of a_1' and the contraction of a_2' are not equal and opposite, as would be required by a pure shear x_y. The crystal shows in addition to the shear x_y, a distortion which is about an order of magnitude smaller than x_y and which turns out to be proportional to the square of the spontaneous polarization (see Section 4). The deformation of the insulated crystal coincides perfectly with the mean curve (curve $P = 0$ in Fig. III-9). The experimental results can be expressed in the following way: the expansion of a

single domain crystal along a_1' is

$$x_1' = \frac{b}{2}P + \alpha P^2, \tag{III-3}$$

with $b \cong 2.0 \times 10^6$ c.g.s units, $\alpha = 3.84 \times 10^{-12}$ c.g.s units; and the expansion along c (see Fig. III-7) is

$$x_3 = \beta P^2, \tag{III-4}$$

with $\beta \cong 2.9 \times 10^{-12}$ c.g.s. units.

The dependence of the spontaneous shear x_y upon temperature was determined by de Quervain's X-ray investigation from the data shown in Fig. III-7. The thermal behavior of x_y is strikingly similar to that of the spontaneous polarization, as shown in Fig. III-4, where the triangles refer to the values of the spontaneous shear. Thus, it is evident that the spontaneous *deformation is directly proportional to the spontaneous polarization*. The question that immediately arises is whether the constant of proportionality between these spontaneous quantities in the ferroelectric region is the same as that occurring in the piezoelectric effect above the transition temperature. The answer can be given only after studying the piezoelectric behavior of the crystal above T_c, which we are going to do in the next section, and is significantly affirmative. For the time being, we limit ourselves to stating that de Quervain's data yield the following value for the proportionality constant between spontaneous deformation and polarization (at 110 °K):

$$\frac{P_s}{x_y} = 6.15 \times 10^{-4}\ \text{C/cm}^2 = 1.85 \times 10^6\ \text{c.g.s units}. \tag{III-5}$$

4. Piezoelectric and Elastic Properties

The definition of the coefficients which characterize the piezoelectric and elastic properties of a crystal is given by the fundamental equations established in Section I-5, namely Eqs. (I-4a), (I-4b), (I-5a), (I-5b). As mentioned previously, the most convenient set of equations to use from the experimental viewpoint is that involving the stress tensor X and the field vector E as *independent* variables, i.e. Eqs. (I-5b):

$$\left.\begin{aligned} P &= -dX + k^X E, \\ x &= -s^E X + dE. \end{aligned}\right\} \tag{III-6}$$

In the case of KDP, which belongs to the point group $\bar{4}2m$ at room temperature, the scheme of the piezoelectric moduli d_{ik}, referred to the co-ordinate system a_1, a_2, c (see Fig. III-8) has the following form: (C 1)

$$\begin{matrix} 0 & 0 & 0 & d_{14} & 0 & 0 \\ 0 & 0 & 0 & 0 & d_{14} & 0 \\ 0 & 0 & 0 & 0 & 0 & d_{36} \end{matrix}$$

Thus, there are only two non-zero piezoelectric moduli, d_{14} and d_{36}.

The non-zero dielectric susceptibilities are of course $k_{11}^X = k_1^X = k_a^X$ and $k_{33}^X = k_3^X = k_c^X$, and the scheme of the elastic compliances s_{ik}^E is (neglecting the superscript E):

$$\begin{matrix} s_{11} & s_{12} & s_{13} & 0 & 0 & 0 \\ s_{12} & s_{11} & s_{13} & 0 & 0 & 0 \\ s_{13} & s_{13} & s_{33} & 0 & 0 & 0 \\ 0 & 0 & 0 & s_{44} & 0 & 0 \\ 0 & 0 & 0 & 0 & s_{44} & 0 \\ 0 & 0 & 0 & 0 & 0 & s_{66} \end{matrix}$$

thus involving only six non-zero coefficients.

The experimental evidence (to be discussed below) shows that some of the piezoelectric moduli, d_{ik}, and elastic compliances, s_{ik}^E, behave anomalously at the Curie temperature. This is in accordance with Eq. (I-6). We may now make a step further and ask: which one of the coefficients d_{ik} and s_{ik}^E is going to behave anomalously as the transition temperature is approached? The answer is that anomalies may occur for those piezoelectric and elastic coefficients which are related to the polarization along the ferroelectric direction. These are, in the present case of KDP: the piezoelectric modulus d_{36}, which relates the shear stress $X_y = X_6$ to the polarization $P_c = P_3$; and the elastic compliance s_{66}^E, which relates the shear stress X_6 to the shear deformation $x_y = x_6$. Eq. (III-6) can be specified in this case, thus:

$$\left.\begin{aligned} P_3 &= -d_{36}X_6 + k_3^X E_3, \\ x_6 &= -s_{66}^E X_6 + d_{36}E_3. \end{aligned}\right\} \tag{III-7}$$

Piezoelectric Properties

From the first of Eqs. (III-7), we see that if $E = 0$, then $P_3 = d_{36}X_6$, and we can therefore measure the modulus d_{36} by applying a known stress X_y to the crystal and measuring the polarization P_3 induced piezoelectrically on the c faces of the crystal. Such measurements were carried out by Bantle and Caflish (B 7).

On the other hand, from the second of Eqs. (III-7), we see that $x_6 = d_{36}E_3$, if $X_6 = 0$. Thus, if we apply a field E_3 on the stress-free crystal and measure the piezoelectric strain, x_y, we again have a way to determine d_{36}, in this case from the converse piezoelectric effect. Such measurements were carried interferometrically by von Arx and Bantle (V 1).

The results of both the measurements of the direct and the converse piezoelectric effect are in excellent agreement with each other, as required by thermodynamics, and yield the temperature dependence of the modulus d_{36} which is depicted in Fig. III-10. It follows from the results that d_{36} obeys a Curie–Weiss law of the type:

$$d_{36} = d_{36}^0 + \frac{B}{T - T_0} \tag{III-8}$$

where $B = 1.26 \times 10^{-4}$ c.g.s. units, $d_{36}^0 \cong -8 \times 10^{-8}$ c.g.s. units and $T_0 = T_c$. The temperature-independent constant d_{36}^0 can, however, be neglected in the vicinity of the Curie temperature. It is evident from Fig. III-10 that the piezoelectric modulus d_{36} shows a marked anomaly at the transition temperature.

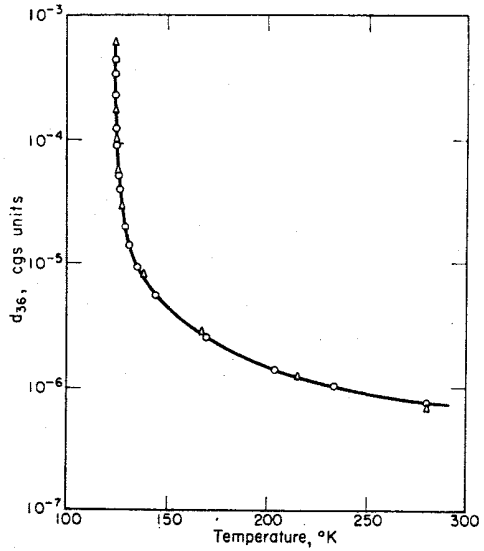

FIG. III-10. Piezoelectric modulus d_{36} of KDP as a function of temperature according to the measurements of the direct effect (triangles) and the converse effect (open circles) (according to Bantle and Caflish (B 7) and von Arx and Bantle (V 1)).

The first important consequence of this result is the following. We see from Eqs. (III-7) that, for the stress-free crystal ($X = 0$), the polarization P_3 and the deformation x_y are related in the following way:

$$P_3 = \frac{k_c^X}{d_{36}} x_6 . \qquad \text{(III-9)}$$

Recalling that the dielectric susceptibility also follows a Curie–Weiss law:

$$k_c^X \cong \frac{C}{4\pi(T - T_0)},$$

we can see that the ratio

$$\frac{k_c^X}{d_{36}} \cong \frac{C}{4\pi B} = 2.05 \times 10^6.$$

This value has the same order of magnitude as in normal piezoelectric crystals, e.g. quartz. Moreover, this value is very close to the value determined by de Quervain (D 2) for the ratio between the *spontaneous* polarization P_s and the *spontaneous* strain x_y below the transition temperature (Eq. III-5). The value of k_c^X/d_{36} is very slightly temperature dependent, as shown in Fig. III-11, whence it appears that de Quervain's result fits perfectly on the extrapolation of the line

below the transition point. Thus, we conclude that the proportionality between polarization and deformation, a fundamental property of all piezoelectric crystals, is not disturbed by the onset of ferroelectricity. *The piezoelectric anomalies are only a consequence of the dielectric anomalies.*

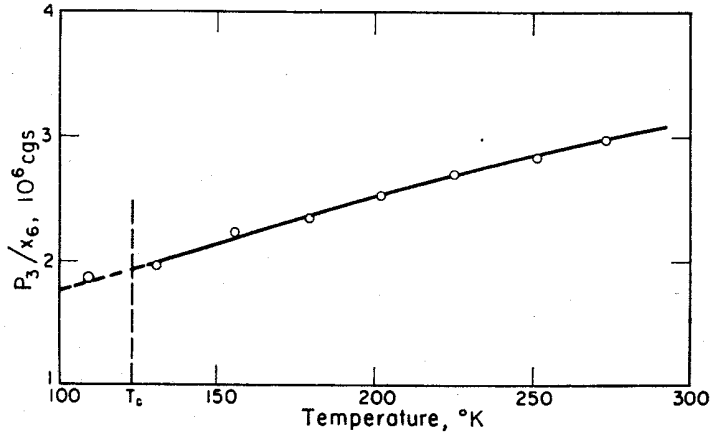

FIG. III-11. Temperature dependence of the ratio between polarization $P_3 = P_s$ and shear strain $x_6 = x_y$ in KDP at zero stress (according to de Quervain (D 2)). The experimental points above the Curie point T_c were calculated from the ratio (k_3^X/d_{36}) between the dielectric susceptibility of the free crystal along c (k_3^X) and the piezoelectric modulus d_{36}. The point below T_c was determined from the ratio between *spontaneous* polarization and *spontaneous* strain, as measured with X-rays.

Very closely above the transition temperature, therefore, non-linearity of the piezoelectric modulus and saturation effects are observed (V 1), which are fully analogous to those exhibited by the dielectric constant (B 4) (see Section 3). In the ferroelectric region, on the other hand, the relation between piezoelectric polarization and stress is no longer unique. If we apply large enough stresses to displace the domain walls, we can observe a *piezoelectric hysteresis* curve (V 1). The direct measurement of d_{36} below the transition point can, therefore, only be carried out on a single-domain crystal. If the measurement is to be carried out via the determination of the strain caused by an applied field E_3, care should be exercised to correct for the so-called *quadratic piezoelectric effect*. This effect arises because the symmetry of the crystal is lowered in the polar phase, so that new piezoelectric moduli come into being. As this effect is inherent to all ferroelectric crystals in their polar phases, we discuss it in some detail in the following.

The actual measurement of the piezoelectric strain x_y is carried out indirectly by determining the elongation along the [110] direction, or, in other words, the elongation along the a_1' axis as discussed in connection with Fig. III-8. Calling this elongation x_1', it can be shown that, above the Curie point, $x_1' = x_y/2$. In this respect, it is easier to refer the properties to the primed co-ordinate system a_1' and c rather than to a_1 and c. In the new system, the scheme of the piezoelectric

moduli is written in the following way:

$$\begin{matrix} 0 & 0 & 0 & 0 & d'_{15} & 0 \\ 0 & 0 & 0 & -d'_{15} & 0 & 0 \\ d'_{31} & -d'_{31} & 0 & 0 & 0 & 0 \end{matrix}$$

and it is the modulus d'_{31} which is going to be anomalous at the transition temperature. It is: $d'_{31} = d_{36}/2$ and $x'_1 + x'_2 = 2x'_1 = x_6$.

Below the transition point, the symmetry is orthorhombic, point group mm, and the corresponding scheme of the piezoelectric moduli is

$$\begin{matrix} 0 & 0 & 0 & 0 & d''_{15} & 0 \\ 0 & 0 & 0 & d''_{25} & 0 & 0 \\ d''_{31} & d''_{32} & d''_{33} & 0 & 0 & 0 \end{matrix}$$

Thus, we see that $d''_{31} \neq d''_{32}$, and then $x''_1 \neq x''_2$, and x''_1 is no longer equal to $x_y/2$. Moreover, a new non-zero modulus appears, d''_{33}; the polarization P_3 can be affected by a pressure along the c axis. The occurrence of these moduli represents simply the normal (linear) piezoelectric effect of the low-symmetry phase, but it is called the quadratic piezoelectric effect of the higher-symmetry phase because these new moduli are proportional to the polarization. Written in terms of polarization P (Eq. I-4b), the elongation x'_1 of a single domain crystal takes the form

$$x'_1 = \frac{b_{36}}{2} P_3 + \alpha P_3^2.$$

This explains the results obtained for the expansion of an *insulated* crystal in the ferroelectric region (Fig. III-9 and Eq. (III-3)) as being due to the quadratic piezoelectric effect. The insulated crystal splits into equal volumes of positive and negative domains and only the quadratic effect can be detected.

Before closing this discussion of the piezoelectric properties of KDP, it should be pointed out, in connection with Eq. (III-9), that several interesting conclusions can be drawn from the fact that the ratio k_c^X/d_{36} is almost temperature independent. Since according to Eq. (I-6), $k^X/d = b$, the piezoelectric coefficient b_{36} must be practically temperature independent. Moreover, as the difference between clamped and free dielectric susceptibility is also independent of temperature, Eq. (III-1) ($\chi^x - \chi^x = ab$) predicts that the corresponding coefficient a_{36} is also practically independent of temperature. For this reason, the coefficients a and b are often called the "true" constants of the piezoelectric crystal, expressing the fact that the "true" piezoelectric behavior of the crystal is normal throughout the ferroelectric transition.

The behavior of the piezoelectric modulus d_{14} is also interesting. This modulus relates the shear stress $Y_z = Z_y = X_4$ to the polarization in the a direction P_1. Since the dielectric constant ε_a has a small anomaly at the transition temperature (Fig. III-1), the modulus d_{14} is also expected to behave anomalously. Figure III-12 shows that this is in fact the case.

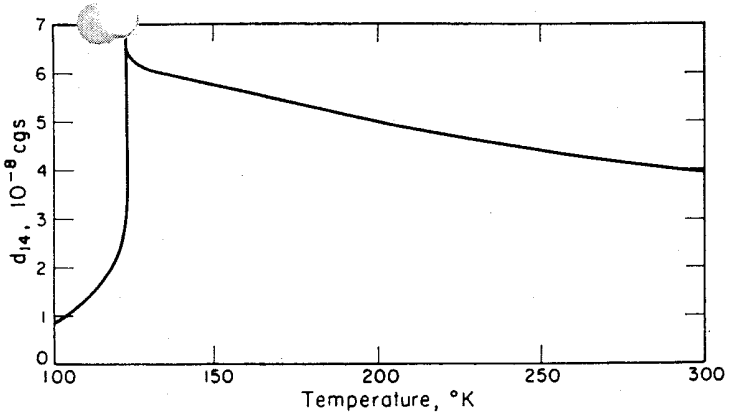

FIG. III-12. Temperature dependence of the piezoelectric modulus d_{14} of KDP (according to Ess (E 1)).

Elastic Properties

Turning now to the elastic properties of KDP, we are in the position to predict what anomalies will occur. We know that, if $E = 0$, a relatively small shear stress X_y causes a very large polarization P_3 along the c axis shortly above the Curie point (d_{36} is very large). We know also that this polarization P_3 is proportional to the shear strain x_y. Thus, a relatively small shear stress X_6 causes a very large shear deformation x_6 in the vicinity of the transition point. Since, from (III-7), $x_6 = s_{66}^E X_6$, it follows that the elastic compliance at constant (zero) field must show a large anomaly at the transition, similarly as do ε_3 and d_{36}. This anomaly is therefore a direct consequence of the anomalous piezoelectric properties and, in the final instance, of the anomalous dielectric properties.

The condition $E = 0$ is very important. It is experimentally fulfilled by coating the c faces of a KDP plate with conducting material and shorting the two electrodes. Accordingly, the behavior of the crystal at $E = 0$ is often referred to as that of the *shorted* crystal. With respect to the shear X_6, the shorted crystal becomes very *soft* in the vicinity of the transition point.

The experimental method consists in measuring the resonance frequency of suitable plates and bars excited piezoelectrically. It can be shown (M 1) that the resonance frequency ν_R is proportional to $1/l\sqrt{(\varrho s_{66})}$, where l is the length and ϱ the density of the crystal bar.

If, on the other hand, the condition $E = 0$ is not fulfilled, i.e. the crystal is *insulated*, then the polarization P_3 caused by a shear X_6 induces charges on the c faces of the crystal. These charges, in turn, cause a strong depolarizing field $E_3 = -4\pi P_3$, which reduces the polarization practically to zero. The *insulated* crystal corresponds to the condition $D = 0$, where D is the dielectric displacement. In ferroelectric crystals, owing to the large values of the dielectric constant, the condition $D = 0$ is practically the same as the condition $P = 0$.

In this case, according to Eq. (I-4b) ($x_6 = -s^P_{66}X_6$), we measure the elastic compliance at constant (zero) polarization. Since the polarization is suppressed, the strain x_6 caused by the stress X_6 will remain normally small and the compliance s^P_{66} will have no anomaly at the transition temperature. The *insulated* crystal remains *hard* through the ferroelectric transition. The compliance s^P_{66} is a "true" constant in the sense introduced above for the piezoelectric coefficients a and b.

Experimentally, the compliance s^P_{66} can be measured by exciting vibrations of the unplated crystal in the wide gap of a condenser (B 4). Let t_g be the total thickness of the gap between the condenser plates and the surface of the crystal plate, and t_c the thickness of the crystal plate. As the condenser plates are short-circuited, we can write:

$$t_g E_g + t_c E_c = 0,$$

where E_g and E_c are the field strengths across the gap and the crystal, respectively. The continuity of the dielectric displacement at the crystal surfaces requires that:

$$E_g = E_c + 4\pi P.$$

Eliminating E_g from the two above equations and introducing into (III-7), we obtain

$$x_6 = \left[s^{E=0}_{66} - \frac{4\pi d^2_{36}}{\varepsilon_3 + \frac{t_c}{t_g}} \right] X_6,$$

and the expression in the brackets can be looked upon as being the elastic compliance of the crystal in a gap. Letting the gap thickness t_g go to infinity ($t_g \to \infty$), we obtain the elastic compliance of the insulated crystal:

$$s^{\text{insulated}}_{66} = s^{E=0}_{66} - \frac{4\pi d^2_{36}}{\varepsilon_3} = s^P_{66}. \qquad \text{(III-10)}$$

The latter equality can be derived directly from Eqs. (I-4a)–(I-5b). In the vicinity of the transition temperature, where $\varepsilon_3 > 10^3$, by choosing a gap such that $t_g = t_c$ we actually measure s^P, since the error involved becomes smaller than 0.1% (B 4).

However, if the frequency of the mechanical vibrations of the crystal becomes very high, the pattern of the surface charges generated piezoelectrically may be such as to reduce the depolarizing field even if the crystal is electrically insulated. Another method used for the determination of the elastic constants of ferroelectric crystals consists, namely, in exciting the crystal to very high-frequency vibrations (~20 Mc/s) by means of an external transducer. The ultrasonic waves travelling within the crystal give rise to local variations of the refractive index and represent, therefore, a sort of three-dimensional grating which causes diffraction of a monochromatic light beam sent through the crystal. This is the method of Schäfer–Bergmann (B 8), (Z 1), (J 1). In this case, the sample is unplated, but it can be shown that the elastic constants determined with this method approach the values of the shorted crystal as the measuring frequency is increased (J 1).

The experimental results of the elastic measurements show very nicely the difference between s^P_{66} and s^E_{66}. Figure III-13 depicts the result of Mason's resonance investigation (M 2). The coefficients reported in the figure are the elastic constants c^E_{66} and c^P_{66} ($= 1/s^P_{66}$). It is easy to show from Eqs. (I-4a) to (I-5b) that $s^E_{66} = 1/c^E_{66}$ and, of course, $s^P_{66} = 1/c^E_{66}$. The analysis of the data reported graphically in Fig. III-13 shows that a Curie–Weiss law holds for the quantity $s^E_{66} - s^P_{66}$:

$$s^E_{66} - s^P_{66} = \frac{D}{T - T_0}, \qquad \text{(III-11)}$$

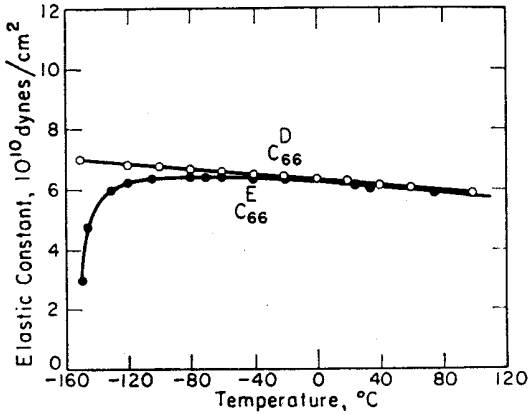

FIG. III-13. Elastic constants c^E_{66} and c^D_{66} ($= c^P_{66}$) of KDP as a function of temperature (according to Mason (M 2)).

where $D = 4.6 \times 10^{-11}$ cm^2 °C/dyn and T_0 is again the transition temperature T_c. This elastic Curie–Weiss law is to be expected from Eq. (III-10), whence taking into account the piezoelectric Curie–Weiss law (III-8) and the dielectric Curie–Weiss law, it follows that

$$D = \frac{4\pi B^2}{C}. \qquad \text{(III-11a)}$$

From this, the expected value of D is 6.1×10^{-11} cm^2 °C/dyn. This value is in satisfactory agreement with the value of the elastic Curie constant measured directly, if we take into account the experimental accuracy.

It should also be pointed out that the dynamic method often used for the determination of the elastic (and piezoelectric) coefficients makes it necessary to distinguish between adiabatic and isothermal conditions, just as in the case of the dielectric constant. This problem was also investigated by Baumgartner (B 4). The ratio between isothermal and adiabatic values of the piezoelectric or elastic coefficients is equal to that between isothermal and adiabatic dielectric constants (see Section II-5).

The elastic properties of KDP which are not related to the anomalous shear in the (001) plane are quite normal. Figure III-14 shows the thermal behavior of the c_{ik} constants (except c_{66}) measured by Zwicker (Z 1) with the Schäfer–Bergmann method. The c_{ik} coefficients (or "elastic constants") are defined in Eqs. (I-4a) and (I-5a), and their matrix is equal to that of the s_{ik}. The indeterminacy of the constants c_{11} and c_{33}, below the transition temperature, is due to the lower-

ing of the symmetry in the ferroelectric phase. The small anomaly of the c_{12} constant is not reliable, owing to the large experimental error involved in the measurement of this coefficient.

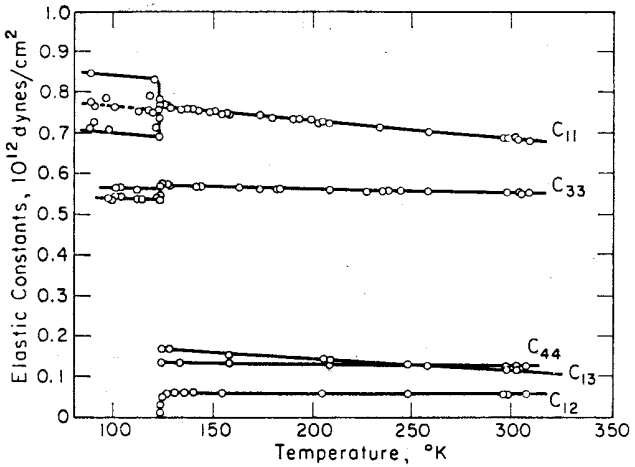

FIG. III-14. Elastic constants c_{ik} (except c_{66}) of KDP as a function of temperature (according to Zwicker (Z 1)).

The "True" Constants

What are now the conclusions that can be drawn from the study of both the piezoelectric and elastic properties of KDP? We have learned that some of the coefficients d_{ik} and s^E_{ik} (and c^E_{ik}) behave anomalously at the transition temperature (piezoelectric and elastic Curie–Weiss laws) and that these anomalies are consequences of the dielectric anomaly (dielectric Curie–Weiss law). We have also learned that both the piezoelectric coefficients a_{ik} and b_{ik}, as well as the elastic quantities at constant polarization, s^P_{ik} and c^P_{ik}, do *not* exhibit anomalies at the Curie temperature. It is, therefore, more logical, for theoretical considerations, to describe the properties of KDP in terms of the system of Eqs. (I-4a) and (I-4b), involving "true" constants of the crystal; namely

$$\left.\begin{aligned} X_6 &= -c^P_{66}x_6 + a_{36}P_3, \\ E_3 &= -a_{36}x_6 + (1/k^x_3)P_3, \end{aligned}\right\} \qquad \text{(III-12)}$$

and:

$$\left.\begin{aligned} x_6 &= -s^P_{66}X_6 + b_{36}P_3, \\ E_3 &= b_{36}X_6 + (1/k^X_3)P_3. \end{aligned}\right\} \qquad \text{(III-13)}$$

In the latter system, it is only the susceptibility k^X_3 of the free crystal which behaves anomalously; in the former, it is the susceptibility k^x_3 of the clamped crystal. For convenience, a list of the anomalous and non-anomalous coefficients and their interelations is presented in Table III-2.

The relation between the reciprocal free- and clamped-susceptibilities was already given in Eq. (III-1). We see from this equation that since $a = d/k^X s^P$ and $b = as^P$, we can write:

$$\frac{1}{k^x_3} = \frac{1}{k^X_3} + \frac{(d_{36})^2}{(k^X_3)^2 s^P_{66}}.$$

Hence, if we assume that a Curie–Weiss law holds for the free susceptibility, namely that $k^X_3 = (C/4\pi)/(T - T_0)$, we are led, after several steps, to a Curie–Weiss law for the clamped crystal (B 13):

$$k^x_3 = \frac{(C/4\pi)}{T - [T_0 - \{(d_{36})^2 C/4\pi (k^X_3)^2 s^P_{66}\}]}. \qquad \text{(III-14)}$$

Thus, we see that the Curie constant remains the same, and the transition of the clamped crystal is predicted to be lower by the amount

$$(d_{36})^2 C/4\pi (k^X_3)^2 s^P_{66}.$$

This factor is independent of temperature and is computed to be approximately 4°, in agreement with the experimental results reported in Section 2. Thus, the effect of clamping is to reduce the range of the ferroelectric state.

The transition of the free crystal occurs when $\chi^X_3 = 1/k^X_3$ becomes equal to zero, i.e. from Eq. (III-1), when the reciprocal susceptibility of the clamped crystal becomes equal to

$$\chi^x_3 = \frac{1}{k^x_3} = a_{36}b_{36} = \frac{(d_{36})^2}{(k^X_3)^2 s^P_{66}},$$

TABLE III-2. ANOMALOUS AND NON-ANOMALOUS ("TRUE") COEFFICIENTS OF FERROELECTRIC CRYSTALS THAT ARE PIEZOELECTRIC IN THE NON-POLAR PHASE

	Piezoelectric–Elastic equations	
	$P = -dX + k^X E$ $x = -s^E X + dE$ $P = ex + k^x E$ $X = -c^E x + eE$	$E = bX + \chi^X P$ $x = -s^P X + bP$ $E = -ax + \chi^x P$ $X = -c^P x + aP$

	Anomalous coefficients			Non-anomalous coefficients
	General symbol	KH_2PO_4	Rochelle salt	
Dielectric	k^X, k^x	k^X_3, k^x_3	k^X_1, k^x_1	
Piezoelectric	d, e	d_{36}, e_{36}	d_{14}, e_{14}	b, a
Elastic	c^E, s^E	c^E_{66}, s^E_{66}	c^E_{44}, s^E_{44}	c^P, s^P

Relations between the coefficients	
$\chi^X = 1/k^X$, $\chi^x = 1/k^x$ $d = es^E$ $c^E = 1/s^E$ $k^X - k^x = ed$	$b = as^P$ $c^P = 1/s^P$ $\chi^x - \chi^X = ab$
$d/k^X = b$ $e/k^x = a$ $s^E - bd = s^P$	

which corresponds to a dielectric constant of approximately [illegible] K 4).

In conclusion, since the piezoelectric and elastic anomalies of KDP are consequences of the dielectric anomaly of the clamped crystal, it is clear that a successful theory of the ferroelectric effect in KDP should have as its first aim an explanation of the latter anomaly only.

5. Optical Properties and Electro-optic Effect

KDP crystals are negative uniaxial. The refractive indices for the sodium *D* lines are, at 15 °C, $n_1 = n_2 = n_o = 1.5095$ and $n_3 = n_e = 1.4684$. The birefringence ($n_3 - n_1 = 0.0411$) is larger than that of quartz (0.0091) but smaller than that of calcite (0.1721). The birefringence increases with decreasing temperature and shows an anomaly at the transition point (Z 2) (see Fig. III-16). This anomaly is due to the so-called "spontaneous Kerr effect" resulting from spontaneous strain and polarization *via* piezo-optic and electro-optic effects. These effects are usually very small in normal crystals but become large enough to be observed in ferroelectric crystals. We therefore give in the following a concise treatment of these effects with special reference to the case of KDP. The theory originates from Pockels (P 1) and is reported briefly in Cady's book (C 1).

It is well known that the optical properties of a crystal are characterized by the index-ellipsoid, or indicatrix, defined as

$$\frac{x^2}{n_1^2} + \frac{y^2}{n_2^2} + \frac{z^2}{n_3^2} = 1, \qquad \text{(III-15)}$$

where n_1, n_2, n_3 are the principal refractive indices. The optical properties of any substance can be affected by external mechanical stresses: this is the effect of *photoelasticity*, which, in crystals, is usually called the *elasto-optic* or *piezo-optic effect* and occurs in *all* crystals. In addition, in crystals which belong to a non-centrosymmetrical point group, the optical properties, viz. the refractive indices, can be affected by external electric fields. This is the *electro-optic* effect. Both the piezo-optic and the electro-optic effect consist in a distortion of the indicatrix (III-15) under the influence of mechanical or electrical stresses. The equation of the deformed indicatrix is, generally:

$$a_{11}x^2 + a_{22}y^2 + a_{33}z^2 + 2a_{23}yz + 2a_{31}zx + 2a_{12}xy = 1 \qquad \text{(III-16)}$$

where the a_{ik}'s (not to be confused with the piezoelectric constants of Eq. (I-4a)) are called the *polarization constants*. The theoretical treatment of the piezo-optic and electro-optic effect, as given by Pockels, consists of expressing the *change* in the polarization constants in terms of the strains x_{jl} and the polarization P, thus:

$$a_{ik} - \delta_{ik}\frac{1}{n_i^2} = \sum_1^3 p_{ikjl}^P x_{jl} + \sum_1^3 r_{ikj}^x P_j \qquad \text{(III-17)}$$

where δ_{ik} is the Kronecker symbol, the p_{ikjl}^P are the piezo-optic coefficients at constant polarization and r_{ikj}^x are the electro-optic coefficients at constant strain. The three equations (III-17) for which the Kronecker symbol is equal to 1 (δ_{ii})

represent a ch[illegible] in length of the principal axes of the indicatrix, the remaining three equations (for which $\delta_{ik} = 0$) represent a rotation of the indicatrix around its axes.

For experimental purposes, it is better to express the change of the polarization constants in terms of stress X and field E. We do this in two steps. First we write the change of the polarization constants in terms of strain and field:

$$a_{ik} - \delta_{ik}\frac{1}{n_i^2} = \sum_1^3 p_{ikjl}^E x_{jl} + \sum_1^3 e_{ikj}^x E_j. \qquad \text{(III-18)}$$

The first term on the right-hand side represents the piezo-optic effect; the second term represents the electro-optic effect, occurring only in non-centrosymmetrical classes. The electro-optic coefficients e_{ikj}^x are, however, not accessible to direct measurements, because an external electric field E causes elastic deformations as a consequence of the piezoelectric effect and the electrostriction, and these deformations, in turn, affect the refractive indices through the piezo-optic effect.

The second step consists of replacing the strains with the stresses and the fields. An expression for the strains in terms of X and E can be obtained from the fundamental expansion of the free energy $A(X, E)$ (Eq. I-3b). Dropping subscripts and summation signs for the sake of simplicity, we obtain for the strains:

$$x = -sX + dE + ME^2. \qquad \text{(III-19)}$$

Substituting (III-19) into (III-18), we obtain

$$a - \delta_{ik}\frac{1}{n^2} = -psX + (e + pd)E + pME^2 = -gX + fE + hE^2, \qquad \text{(III-20)}$$

In the most general case (triclinic symmetry), we will have thirty-six non-zero piezo-optic constants $g = ps$; eighteen electro-optic moduli of the *first order* $f = e + pd$; and thirty-six electro-optic moduli of the *second order* $h = pM$. In the special case of KDP, there are only two non-zero electro-optic moduli of the first order, namely f_{41} and f_{63}, and seven non-zero electro-optic moduli of the second order, namely h_{11}, h_{12}, h_{13}, h_{31}, h_{33}, h_{44} and h_{66}. The equation of the indicatrix can now be written by replacing the polarization constants from (III-20) into (III-16).

In practice, this equation can be considerably simplified, as it was done in the case of KDP by Zwicker and Scherrer (Z 2). The measurements were carried out on the stress-free crystal ($X = 0$) and the second-order piezoelectric effect could be neglected in all temperature ranges except very close to the transition point. Under these conditions, the equation of the indicatrix can be written as:

$$\frac{x^2 + y^2}{n_1^2} + \frac{z^2}{n_3^2} + 2f_{41}(yE_1 + xE_2)z + 2f_{63}xyE_3 = 1, \qquad \text{(III-21)}$$

where the variables x, y, z are referred to the principal axes a_1, a_2, c of the crystal according to the choice discussed in connection with Fig. III-8. With Eq. (III-21), we are in the position to discuss all electro-optical effects of the first order in KDP.

The most important effect is that obtained by the application of a field E_3 along the tetragonal c axis: $E_1 = E_2 = 0$. In this case, it is clear from (III-21) that the length of the principal axes of the indicatrix along the crystallographic axes a_1, a_2, and c is unchanged by the field. This means that if we send light in the direction of a_1 or a_2 we will not be able to observe a first-order electro-optic effect. However, if we send light in the direction of the tetragonal axis c, we will be able to notice that the field along c has caused an elongation of the a_1' axis and a contraction of the a_2' axis (Fig. III-8). It is therefore more convenient to rewrite the equation of the indicatrix as referred to the coordinate system a_1', a_2', c introduced in Fig. III-8, thus:

$$\frac{x'^2}{n_1^2}(1 + f_{63} E_3 n_1^2) + \frac{y'^2}{n_1^2}(1 - f_{63} E_3 n_1^2) + \frac{z^2}{n_3^2} = 1. \qquad \text{(III-22)}$$

We can easily derive from this equation the birefringence induced by the field in the $a_1' a_2'$ plane:

$$n_{a_1'} - n_{a_2'} \cong n_1^3 f_{63} E_3. \qquad \text{(III-23)}$$

Since, in this experiment, the light beam is parallel to the electric field, one speaks of a *longitudinal* electro-optic effect.

If, on the other hand, the light beam is sent in the direction of the a_1' or a_2' axis, i.e. perpendicular to the field (*transversal* electro-optic effect), Eq. (III-22) yields:

$$\left.\begin{aligned} n_c - n_{a_1'} &\cong (n_3 - n_1) + \tfrac{1}{2} n_1^3 f_{63} E_3, \\ n_c - n_{a_2'} &\cong (n_3 - n_1) - \tfrac{1}{2} n_1^3 f_{63} E_3. \end{aligned}\right\} \qquad \text{(III-24)}$$

Thus, we see that the linear transversal electro-optic effect is superimposed on the natural birefringence of the crystal $(n_3 - n_1)$, and that the effect is half as large as in the case of the longitudinal effect.

If we measure both the longitudinal and the transversal effects as functions of temperature, we have two ways of determining the electro-optic modulus f_{63}, i.e. from (III-23) and (III-24). The experimental results of Zwicker and Scherrer (Z 2) are shown in Fig. III-15. It is evident that f_{63} follows a law of the Curie–Weiss type and is therefore anomalous at the transition. Thus, the ratio f_{63}/ε_3 (where ε_3 is the anomalous dielectric constant along c) is essentially temperature independent. This indicates that, if we had maintained the treatment in terms of polarization P rather than field E (following Eq. III-17), we would have obtained equations involving non-anomalous, "true" electro-optic coefficients. Such equations would also be more significant from the microscopic point of view, since the primary effect on light is certainly given by the polarization of the lattice rather than the externally applied electric field. We write, in other words, that the change in birefringence Δn is proportional to the polarization, thus:

$$\Delta n = \alpha P_3 = \alpha \frac{\varepsilon_3 - 1}{4\pi} E_3,$$

where α is a constant which can be determined experimentally. Comparison of this expression for Δn with (III-23) yields a relation between the dielectric constant ε_c and the electric-optic modulus f_{63} and enables one to "compute"

the dielectric constant from the electro-optic effect. The agreement between computed and observed dielectric constant is quite satisfactory (Z 2) and the small discrepancies are probably due to inaccurate values of the observed dielectric constant.

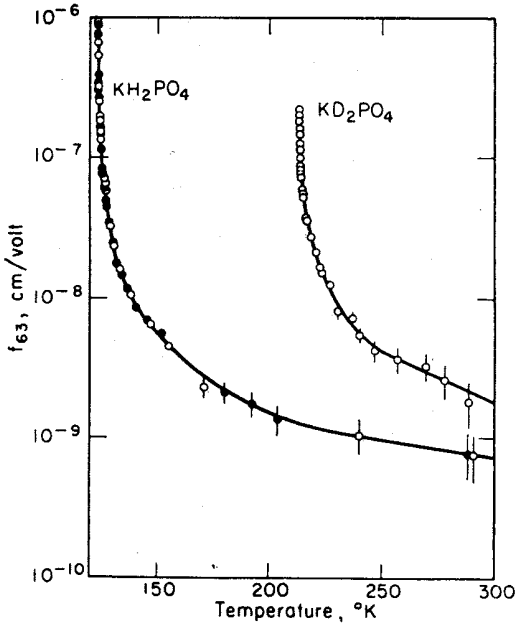

FIG. III-15. Electro-optic modulus f_{63} of KDP as a function of temperature. Open circles: transversal effect; full circles: longitudinal effect (according to Zwicker and Scherrer (Z 2)).

It is interesting to point out, in this connection, that the ratio of f_{63}/ε_3 for KDP is about 1.7×10^{-8} c.g.s., while the same quantity for other piezoelectric crystals, e.g. quartz ($f_{41}/\varepsilon_1 = 1.6 \times 10^{-10}$ c.g.s.), is 100 times smaller. The same order of magnitude is found for the difference between the Kerr effect of polar liquids and that of normal, non-polar liquids. This may indicate that the mechanism of dielectric polarization in KDP differs considerably, even above the transition point, from that of normal crystals (K 4).

In the vicinity of the transition temperature, Zwicker and Scherrer observed pronounced deviations from the expected linear effect described by Eqs. (III-23) and (III-24). These deviations are due to effects which arise in part from the saturation effects of the dielectric constant (see Section 2) and in part from the second-order electro-optic effect superimposed upon the first-order effect discussed above.

Below the transition, the onset of spontaneous polarization along the c axis causes the occurrence of a spontaneous electro-optic effect. The spontaneous change in birefringence in the $a_1'c$ or $a_2'c$ plane can be observed, if the crystal is made a single domain by means of an external field along c. Figure III-16 shows the experimental results (Z 2). It is significant that, when the crystal is insulated,

it splits into equal volumes of positive and negative domains and the experimental curve coincides with the mean value of the curves for a single positive and a single negative domain. The linear effect is compensated and only the quadratic

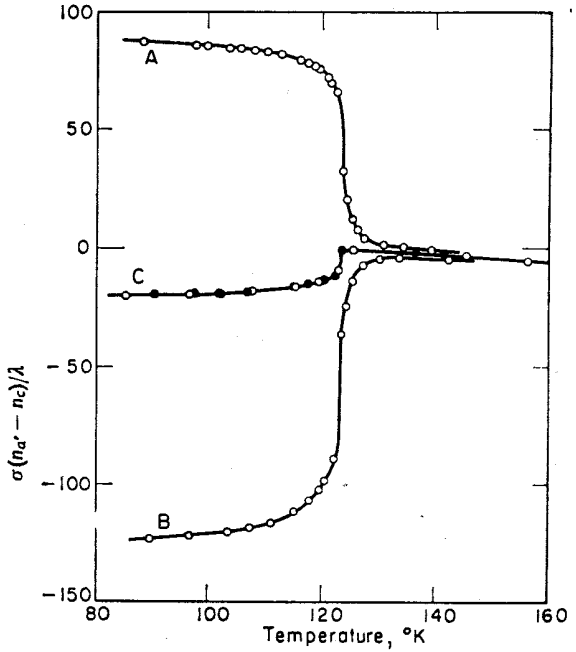

FIG. III-16. Spontaneous change of birefringence $(n_{a'_1} - n_c)/\lambda$ in KDP as a function of temperature. (A) single domain achieved with a bias of +3000 V/cm; (B) single domain achieved with a bias of −3000 V/cm; (C) Mean value of curves (A) and (B) (full circles) and experimental points obtained on insulated crystal (open circles) (according to Zwicker and Scherrer (Z 2)).

effect can be observed. It should be noticed that the same arguments hold for this quadratic effect which are valid for the spontaneous strain (see Section 4); the lowering of the symmetry involves the occurrence of new electro-optic moduli which are proportional to the polarization.

The experiments show that the ratio between the first-order *spontaneous* change in birefringence and the *spontaneous* polarization has the same value as the ratio between the first-order *induced* change in birefringence and the *induced* polarization above the transition temperature. Thus, the electro-optic effect provides a tool for the measurement of the spontaneous polarization. The birefringence shows hysteresis effects in the ferroelectric region (electro-optic hysteresis). Electro-optic measurements also allow one to determine the temperature dependence of the coercive field, the anomaly of the specific heat, etc.

The behavior of the electro-optic modulus f_{41} would, therefore, provide information about the polarization along the tetragonal a axis. However, this

modulus is substantially smaller than f_{63} and its measurement would require the experimental determination of a change in birefringence smaller than 10^{-9}. For this reason, f_{41} could not be measured by Zwicker and Scherrer.

6. Isomorphous Crystals and Isotope Effects

As mentioned in Section 1, a number of crystals isomorphous with KH_2PO_4 also undergo transitions to a phase with lower symmetry at low temperatures. With a very few exceptions, the ferroelectric properties of the low-temperature

TABLE III-3. TRANSITION TEMPERATURES T_c OF CRYSTALS ISOMORPHOUS WITH KH_2PO_4

Substance	T_c (°K)	References
KH_2PO_4	123	V 1
KD_2PO_4	213	B 6
KH_2AsO_4	97	B 6
KD_2AsO_4	162	S 2
RbH_2PO_4	147	M 3, B 16
RbD_2PO_4	218	M 3
RbH_2AsO_4	110	S 2
RbD_2AsO_4	178	S 2
CsH_2PO_4	159	S 3
CsH_2AsO_4	143	S 2
CsD_2AsO_4	212	S 2

phase were confirmed by direct dielectric investigations. In these cases, the behavior was found to be similar to that of KDP.

A very large effect of isotopic substitution (replacement of hydrogen by deuterium) was found in all crystals of this group of ferroelectrics. Table III-3 lists all the ferroelectrics so far investigated in the KDP family. It is seen that the isotope effect consists of a very large change in the transition temperature; the deuterated salts undergo the ferroelectric transition at higher temperatures than the corresponding hydrogen salts, the amount of the displacement of transition temperature varying from 90 °C in KH_2PO_4 to 67 °C in KH_2AsO_4. The magnitude of this isotope effect is an indication of the vital role played by the hydrogen bonds in the mechanism leading to ferroelectricity.

A number of solid solutions between the crystals listed in Table III-3 were studied by Matthias and Merz (M 7). Starting with KH_2PO_4, the Curie temperature is increased by substituting K partially with Tl, while it is decreased when K is partially replaced by Rb, Cs and NH_4. For example, a content of 7.1% Tl in KH_2PO_4 raises the Curie point to 126 °K, a much larger (undetermined) content of Cs in KH_2PO_4 lowers the Curie temperature to 108 °K.

It may be pointed out again here, as mentioned in Section 1, that the ammonium salts of this series of phosphates and arsenates undergo transitions to antipolar states, which we do not discuss in the present book. Large isotope

effects are observed for these transition temperatures as well, namely from -125 °C for $NH_4H_2PO_4$ to approximately -28 °C for $ND_4D_2PO_4$, and from -57 °C for $NH_4H_2AsO_4$ to $+31$ °C for $ND_4D_2AsO_4$. For a general discussion of the properties of these crystals, the reader is referred to the review articles by Shirane *et al.* (S 7), by Känzig (K 4) and to the book of Megaw (M 4).

7. Structural Characteristics

The most important contribution to an understanding of the atomistic mechanism occurring at the ferroelectric transition of KH_2PO_4 came from structural investigations by means of X-ray and neutron diffraction. The first X-ray structural study was done by West (W 2), continued by de Quervain (D 2) and later refined by Frazer and Pepinsky (F 1), who concentrated their attention to the structural changes occurring in a narrow temperature range immediately above and below the transition point. Although the X-ray results gave strong indications as to the location of the hydrogen atoms in the lattice from the interatomic distances between oxygen atoms, it was not until application of neutron diffraction techniques that the hydrogen positions could be accurately located in the structure. The essential role played by neutron diffraction analysis in problems of this sort is due to the difference between the scattering processes of X-rays and neutrons. X-rays are scattered by electrons, thus the scattering factor of the various elements increases with increasing atomic number and is smallest for hydrogen. Neutron scattering, on the other hand, occurs at the nucleus and thus the scattering factors of the chemical elements do not differ much from each other. For details of the neutron diffraction methods, the reader is referred to the book of Bacon (B 9).

Detailed neutron diffraction analyses of KH_2PO_4 were carried out by Bacon and Pease (B 10), (B 11), Peterson *et al.* (P 2) and Levy *et al.* (L 1). The overall picture of the transition occurring in KH_2PO_4 at 123 °K, as obtained both from X-ray and neutron studies, reveals the role played by the hydrogen atoms in the co-operative phenomenon which leads to ferroelectricity. It should be mentioned here that the most successful theory of KH_2PO_4 was developed by Slater (S 4) on a model hypothesized on the basis of the early West's structure (see Section 8). This model assumed the very ordering of the hydrogen atoms which was later beautifully confirmed by the neutron analysis.

The symmetry of the room-temperature phase of KH_2PO_4 is tetragonal. The space group and the dimensions of the unit cell depend on whether we refer it to the coordinate system a_1, a_2, c or a_1', a_2', c of Fig. III-8. In the former case, the space group is $I\bar{4}2d$ and the lattice dimensions are

$$a_1 = a_2 = 7.453 \text{ Å}, \quad c = 6.959 \text{ Å},$$

the unit cell containing four formula units. In the second case, the space group is $F\bar{4}d2$ and the new cell dimensions are:

$$a_1' = a_2' = 10.534 \text{ Å}, \quad c = 6.959 \text{ Å},$$

the cell contains now eight formula units. The latter cell, as we know, remains rectangular below the transition and the space group of the polar orthorhombic phase is Fdd. The changes in cell dimensions with decreasing temperature are summarized in Table III-4.

TABLE III-4. TEMPERATURE DEPENDENCE OF THE LATTICE CONSTANTS OF KH_2PO_4

Temperature (°K)	Space group	Lattice constants (Å)			References
		a	b	c	
295	$F\bar{4}d2$	10.534	–	6.959	B 10
132	$F\bar{4}d2$	10.495	–	6.919	B 11
77	$Fdd2$	10.458	10.540	6.918	B 11
126	$F\bar{4}d2$	10.48	–	6.90	F 1
116	$Fdd2$	10.44	10.53	6.90	F 1

The framework of the room-temperature structure is depicted in Fig. III-17 as obtained from West's data. Each phosphorous atom is surrounded by four oxygens at the corners of a tetrahedron which is almost regular (being compressed by approximately 2% along the c axis). These PO_4 groups, together with the potassium atoms, build up the structure in such a way that K and P atoms alternate each other at a distance $c/2$ in the direction of the c axis. Every PO_4 group is linked to four other PO_4 groups, spaced $c/4$ apart along c, by hydrogen

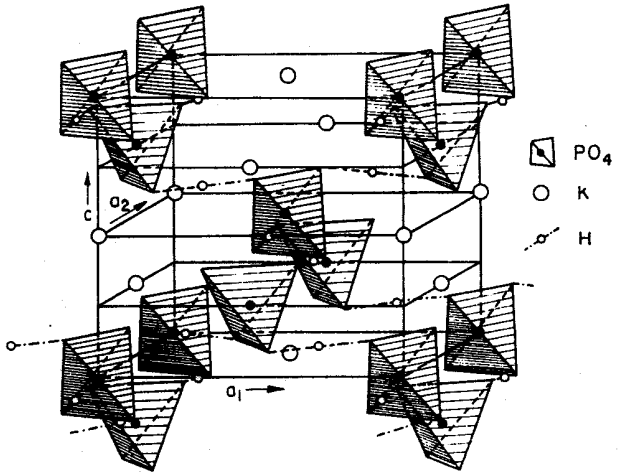

FIG. III-17. Structure of KH_2PO_4. Unit cell in space group $I\bar{4}2d$ (according to West (W 1)).

bonds. Thus, the linkage is such that there is a hydrogen bond between one "upper" oxygen of one PO_4 group and one "lower" oxygen of the neighboring PO_4 group, and each hydrogen bond lies very nearly perpendicular to the c axis.

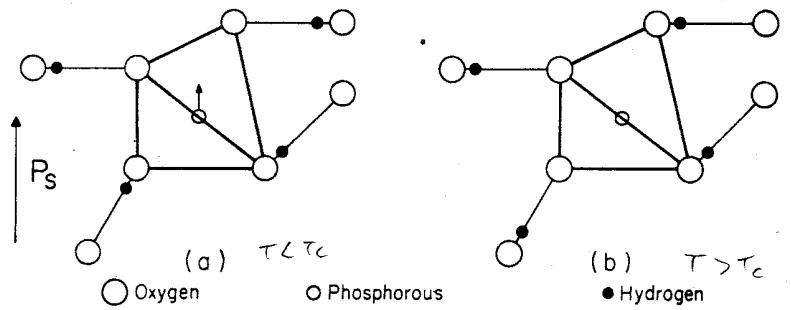

FIG. III-18. Configurations of the $(H_2PO_4)^-$-groups. (a) Dipole moment oriented along the positive c axis. Arrow at the P atom indicates the direction of the shift of this atom below the Curie temperature; (b) No dipole along the c axis.

As revealed by the neutron diffraction studies, only two hydrogens are located nearest any one PO_4 group; therefore, as a group they form $(H_2PO_4)^-$ ions. There are six ways in which two hydrogens can do so, and this gives rise to six different configurations of the H_2PO_4 groups, two when the hydrogens are nearest to both "upper" or both "lower" oxygens and four when the hydrogens are nearest to an "upper" and a "lower" oxygen (Fig. III-18). The PO_4 tetrahedra are also linked by the potassium atoms. Each K is surrounded by eight oxygens and is somewhat closer to four of them than to the other four. The interatomic distances of the room temperature structure are given in the first column of Table III-5 and a schematic projection of the structure on the (001) plane is depicted in Fig. III-19.

Information about the location of the hydrogens in the room temperature structure is given by the Fourier projection on the (001) plane from neutron diffraction data, Fig. III-20(a). The hydrogen nuclei appear as kidney-shaped dotted contours between oxygens of adjacent PO_4 tetrahedra. These contours are elongated along the axis of the bond, a fact that can be explained by either one of the following hypotheses:

(i) the hydrogens perform strong anisotropic vibrations along the bond axis; or

(ii) the hydrogens are distributed statistically off center, the distance between the two positions being about 0.35 Å. The diffraction technique is not able to distinguish between these two alternatives, and a decision must be made on other grounds (see below).

In going through the transition the length of the hydrogen bonds do not change much (Table III-5), but below the transition temperature the hydrogens are ordered in such a way that in a single-domain crystal they are, for example, all near "upper oxygens" or near "lower oxygens", depending on the polarity (see Fig. III-18a). Reversal of the polarity, for example by means of an electric field, produces a shift of the hydrogen atoms along the O–H–O

bonds from one of ordered positions to the other. Figure III-20(b) shows the Fourier projection on (001) at 77 °K. The hydrogen peaks are displaced about 0.20 Å from the center of the O–H–O line. The structure can be looked upon as being built of K atoms and H_2PO_4 groups.

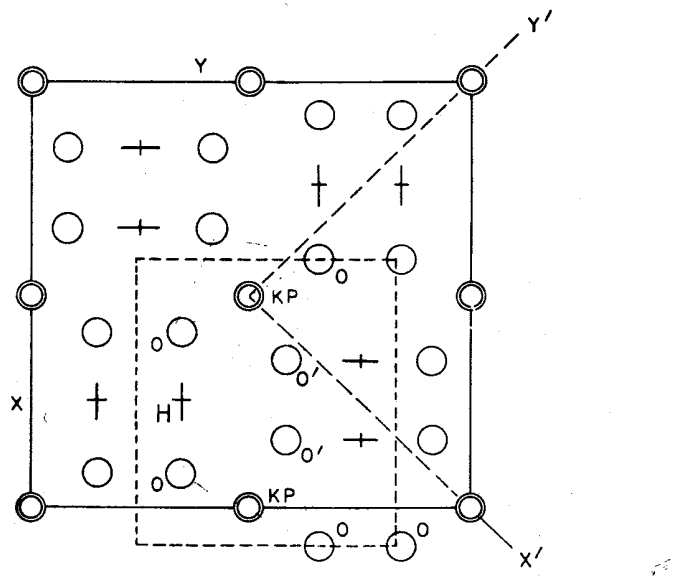

FIG. III-19. Schematic projection of the KH_2PO_4 structure on (001) (according to Bacon and Pease (B 10)).

TABLE III-5. BOND LENGTHS IN KH_2PO_4 [ACCORDING TO BACON AND PEASE (B 11)]

(The lengths have been recomputed in ångström units from the original data (M 4); O_H = oxygen with a close hydrogen.)

Bond	Room temperature	132 °K	77 °K
$P-O_H$ $P-O$	1.541 ± 0.05	1.541 ± 0.004	1.586 ± 0.02 1.511 ± 0.02
O_H-O_H $O-O$	2.533 ± 0.007	2.533 ± 0.009	2.526 ± 0.006 2.554 ± 0.006
$O-O'_H$ O'_H-O	2.508 ± 0.008	2.508 ± 0.005	2.524 ± 0.02 2.517 ± 0.02
$O-H-O$	2.492 ± 0.005	2.480 ± 0.004	2.491 ± 0.004
O_H-H	1.07 ± 0.01	1.07 ± 0.01	1.05 ± 0.014
$O-H$	1.42 ± 0.01	1.41 ± 0.01	1.43 ± 0.014
$K-O_H$ $K-O$	2.894 ± 0.006	2.876 ± 0.003	2.902 ± 0.03 2.839 ± 0.03
$K-O'_H$ $K-O'$	2.825 ± 0.004	2.808 ± 0.005	2.818 ± 0.01 2.783 ± 0.01

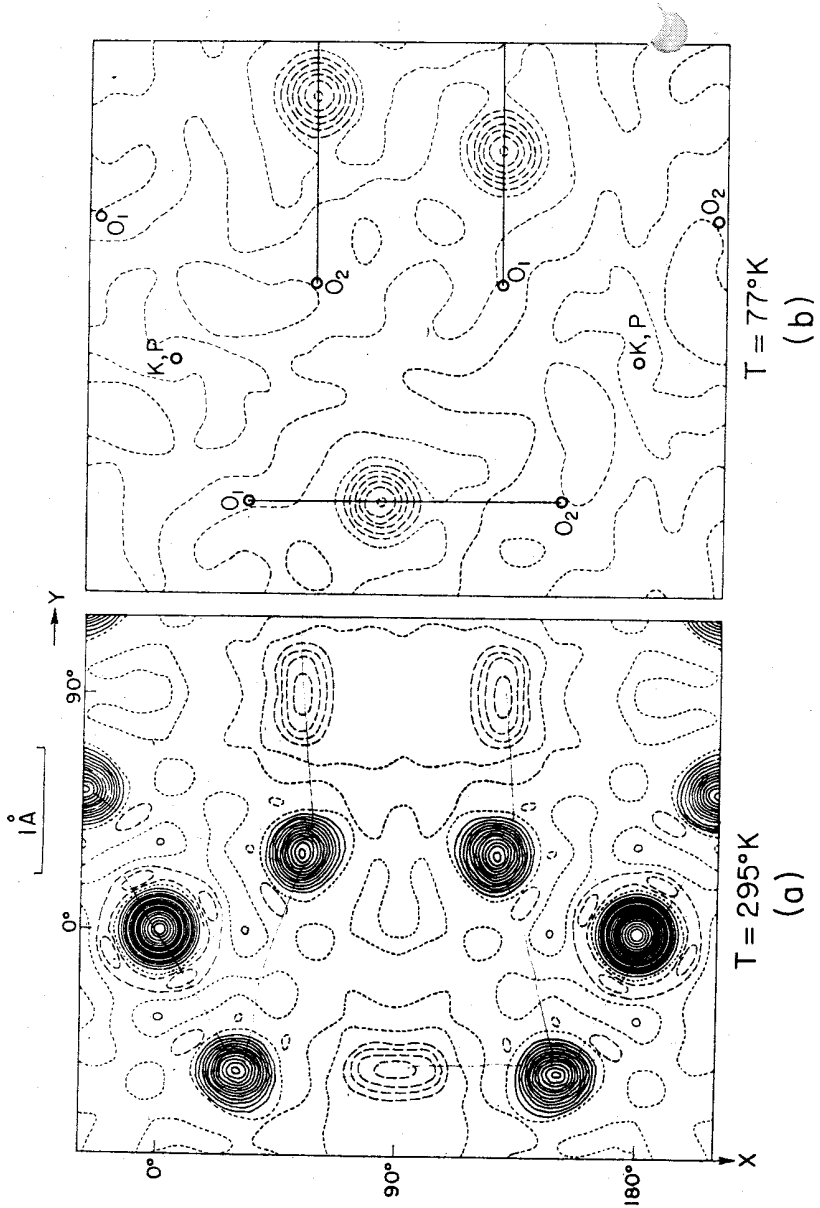

FIG. III-20. Fourier projection on (001) of KH_2PO_4. Solid lines are positive, broken lines negative and dotted lines zero contours. This figure corresponds tothe region outlined by the dotted lines in Fig. III-19 (according to Bacon and Pease (B 10)): (a) at room temperature; (b) at 77 °K, hydrogenatoms only.

This order[illegible] the hydrogen atoms is connected with a significant, although small, shift of the other atoms from their equilibrium position in the tetragonal phase. The overall effect of the transition on the other atoms is the following. The framework of the oxygen atoms is very little affected, except for the small shear of the lattice as a whole. Referred to the oxygen framework, the potassium and phosphorous atoms move along the *c* axis in opposite directions by about 0.01 Å and 0.08 Å, respectively, so that both are farther from those oxygens which have hydrogen atoms close to them (B 11). The X-ray investigation of Frazer and Pepinsky (F 1) yields somewhat different results for the displacement of the potassium and phosphorous atoms, namely 0.05 Å and 0.03 Å in opposite directions, respectively.

Since the hydrogen bonds are only about 0.5° out of parallelism with the (001) plane, the *c* component of the hydrogen shift is far too small to account for the total polarization. Thus, it seems more likely that the polarization arises from the displacements of the potassium and phosphorous atoms in the direction of the *c* axis. We can actually calculate the value of the (ionic) polarization, if we make certain assumptions about the effective charge of each ion in the structure. Assuming for example, such electronic states as P^{5+}, K^{1+} and O^{2-}, we can calculate from the atomic positions reported by Bacon and Pease that the value of the (ionic) spontaneous polarization ought to be 5.0×10^{-6} C/cm². This result is in fairly good agreement with the experimental value $P_s = 4.7 \times 10^{-6}$ C/cm². In the case assumed, the direction of the spontaneous polarization is the same as that of the shift of the P^{5+} ion, as indicated in Fig. III-18(a). More precisely, the polarization is pointing from the oxygen ions that have a hydrogen close to them toward the phosphorous ion. Thus, when the polarization is "up", the hydrogens are nearest to the "lower" oxygens of each PO_4 group.

Bacon and Pease made a different assumption about the electronic states of potassium and phosphorous, namely K^{1+} and P^{3-}. In this way, they calculated a magnitude of 4.7×10^{-6} C/cm² for the spontaneous polarization, which is in better agreement with the experimental data but results in a direction of the spontaneous polarization opposite to that described immediately above. There is admittedly no *a priori* reason for rejecting the model advanced by Bacon and Pease, but their charge assignment is quite difficult to justify.

The ordinary X-ray and neutron analyses are not in a position to give an answer to this problem, as they cannot distinguish between positive and negative directions. The technique based upon the anomalous dispersion of X-rays, however, can do so and it allows the determination of the absolute configuration of polar structures (see Chapter X). The absolute configuration of KH_2PO_4 has recently been determined in this way by Unterleitner *et al.* (U 4). The results of this investigation are in accordance with the first assumption made above, namely that of electronic states K^{1+} and P^{5+}.

Thus, the mechanism of the transition in KH_2PO_4 appears to be rather clearly elucidated by the X-ray and neutron diffraction analyses. Discrepancies between the two methods are found only with regard to the thermal vibrations

of the atoms, in that X-ray evidence seems to point to strong anisotropic vibrations of some atoms (namely K and P), while the neutron data reveal no significant difference, either above or below the transition point, for the amplitude of vibration of any atom in different directions. The latter is true also for the hydrogen atoms, if the elongated peak observed in the (001) projection at room temperature (Fig. III-20a) is assumed to be due to a double minimum potential curve, with half-hydrogen, on the average, in each minimum position.

As stated above, a distinction between the alternatives of anisotropic thermal oscillations and statistical disorder of the hydrogens in the tetragonal phase cannot be made on the basis of the diffraction data alone. The problem has been attacked by the study of infrared and Raman spectra (K 1), (L 2), (L 3), (M 5), (O 1), (R 1). Unfortunately, however, the O–H stretching frequency in crystals containing short hydrogen bonds, such as KDP, is often difficult to identify because of the large frequency displacement and breadth of the bands. In addition, the bands are characterized by low peak intensity, rather flat peaks and often the appearance of several maxima of comparable intensity. These factors make the assignment of a single frequency to the band difficult and somewhat arbitrary. In spite of these difficulties, comparison between the infrared spectra of KH_2PO_4 and KD_2PO_4 led various authors to assign wavenumbers of the order of 2800 cm^{-1} to 2200 cm^{-1} to the hydrogen vibration. Blinc and Hadzi (B 14) gave an interpretation of the particularly interesting spectral region around 2800 cm^{-1} in terms of tunneling of the protons between two minima of potential energy. The minima were taken to be of equal depth in the non-polar phase and unsymmetrical in the ferroelectric phase. A quantum-mechanical treatment of this vibrational problem yielded results which are in agreement with the experimental data.

It should be mentioned, on the other hand, that recent observations, by Pelah *et al.* (P 3), of hydrogen vibration frequencies in KH_2PO_4, by means of inelastic scattering of cold neutrons, indicate that the assignment of the infrared bands around 2800 cm^{-1} to hydrogen vibrations may be questionable. According to the scattering data, it is the infrared reflectance peak at 540 cm^{-1} which should be assigned to the hydrogen vibration mode. However, the information provided by the neutron inelastic scattering data is too scarce, at the present time, to allow a clarification of the contradiction with the infrared results.

The important point is that, irrespective of which of the infrared peak should be identified as due to hydrogen bond vibrations, all infrared and Raman investigation are in accordance in reporting *no change* of the pertinent bonds through the transition point. This means that the O–H···O bond does not change and the O–H···O distances remain essentially the same through the transition. The infrared peaks simply become more intense in the ordered ferroelectric phase.

The infrared measurements, on the other hand, are in agreement in assigning two reflection peaks at about 1100 cm^{-1} and 900 cm^{-1} to the PO_4 vibration (M 5). This is confirmed by the neutron inelastic scattering experiments carried out, for comparison, on K_3PO_4, K_2HPO_4 and KH_2PO_4 (P 3).

Nuclear magnetic resonance experiments also show no significant changes in the line width and relaxation time of the proton magnetic resonance at the transition. Furthermore, recent experiments concerned with the deuteron magnetic resonance spectrum and relaxation on KD_2PO_4 establish that the electric field gradient tensor at the site of the deuteron does not change appreciably with temperature over the transition point (B 12). This indicates again that the nature of the hydrogen bond is not significantly affected by the transition.

8. Theoretical Treatments

The recognition that the anomalies of the piezoelectric, elastic and electro-optic properties of KH_2PO_4 are due, in the final instance, to the anomaly of the dielectric properties of the clamped crystal led the first theoretical efforts toward an explanation of the phenomenon on the basis of *permanent* electric dipoles. The theory of dielectric polarization due to permanent dipoles was developed earlier by Debye from an adaptation of Langevin's theory of paramagnetism to the study of dielectrics. Accordingly, the early theoretical approach to the ferroelectricity of KH_2PO_4 was based on the Langevin-Weiss theory of ferromagnetism. A review of such a treatment can be found in an article by Baumgartner *et al.* (B 13). The interaction between the dipoles was taken into account by way of the Lorentz formula for the internal field: $F = E + \gamma P$, where E is the external field, P the polarization and γ the Lorentz factor. We already know that, if the medium is isotropic or has cubic symmetry, γ has the value $4\pi/3$. In crystals of lower symmetry, γ has values differing from $4\pi/3$, although of the same order of magnitude, and, moreover, it has tensor character. Straightforward application of Boltzmann statistics to an assembly of dipoles in the Lorentz field F leads to the Langevin function and to the prediction of a Curie temperature. However, the quantitative agreement between theory and experiment is so poor that it casts considerable doubt over the validity of Lorentz's internal field concept as a means to express the interaction between the dipoles. The formula of Onsager is a better approximation of this interaction*, but it has

* The explicit assumption made in the Lorentz treatment is that the dipole moments of all atoms are parallel, an assumption which is obviously valid for the *induced* moments in structures with sufficiently high symmetry, but is not valid for *permanent* dipole moments oriented at random. Onsager's model is that of a spherical molecule with radius a and a point dipole μ at its center. The other molecules of the dielectric are treated as a continuum with dielectric costant ε, equal to the actual (unknown) dielectric constant of the substance considered. Onsager's formula is then:

$$\frac{(\varepsilon-1)(2\varepsilon+1)}{12\pi\varepsilon} = \frac{N}{1-f\alpha}\left[\alpha + \frac{\mu^2}{(1-f\alpha)\,3kT}\right],$$

where α is the polarizability and $f = \frac{1}{a^3}\cdot\frac{2(\varepsilon-1)}{2(\varepsilon+1)}$.

This formula can be simplified markedly for the case of negligible polarizability ($\alpha = 0$), thus

$$\varepsilon = \frac{1}{4}\left[\left(1+\frac{4\pi N\mu^2}{kT}\right) + \sqrt{\left\{\left(1+\frac{4\pi N\mu^2}{kT}\right)^2 + 8\right\}}\right],$$

whence one can see, incidentally, that the "$4\pi/3$ catastrophe" is avoided, since $\varepsilon = \infty$ only at $T = 0$.

been shown (P 4) that this formula can only predict a first-order transition from a polar into a non-polar state.

Thus, it appears that the consideration of long-range forces, electrostatic in character, arising from the fields of the dipoles themselves, is insufficient for a quantitatively satisfactory explanation of the ferroelectric phenomenon in KH_2PO_4. A considerably better picture is obtained with Slater's theory (S 4), in which short-range forces provide the entire interaction force. As pointed out previously, Slater's approach is based on the statististical treatment of a model which was derived from West's unrefined structure of KH_2PO_4 long *before* neutron diffraction could prove it correct. Slater's theory represents the first successful attempt to explain the ferroelectricity of KH_2PO_4 from a molecular point of view.

The Theory of Slater

The structural studies (Section 7) have revealed the role played by the hydrogen atoms constituting the bonds which link neighboring PO_4 groups. These PO_4 groups are distributed on a tetragonal diamond-type lattice and each group is surrounded tetrahedrally by four neighboring groups. On every hydrogen bond, there are two equilibrium positions for the hydrogens located symmetrically with respect to the center of the bond. Slater assumes that the distribution of the hydrogens between these positions is subject to two restricting conditions:

(i) There is one and only one hydrogen on each bond.

(ii) There are only two hydrogens near any one PO_4 group.

These two conditions are very similar to those postulated by Pauling for the structure of ice in order to explain its zero-point entropy (P 5). Accordingly, they mean that the structure is built up of $(H_2PO_4)^-$ groups (and K) and that molecular groups such as (H_3PO_4) or $(HPO_4)^{2-}$ are so unlikely to occur that they can be neglected completely. We have seen in the preceding section that there are six possibilities to arrange two hydrogens nearest to a given PO_4 group. Where the two hydrogens are closest to the two "upper" oxygens of the PO_4 group the resulting $(H_2PO_4)^-$ group is considered to be a dipole pointing in the negative direction of the tetragonal c axis; when the two hydrogens are nearest to the "lower" oxygens, the $(H_2PO_4)^-$ dipole points toward the positive end of the c axis; and when one hydrogen is nearest to one "upper" and the other to one "lower" oxygen of the PO_4 group (there being four different ways in which this case can be realized), the $(H_2PO_4)^-$ dipole is oriented perpendicularly to the c axis.

These six configurations are not equivalent. Slater proposes that the two configurations for which either both "upper" or both "lower" oxygens have hydrogens nearest to them (corresponding to dipoles pointing down or up) are energetically equivalent to each other and associated to an energy which is normalized to zero. The remaining four configurations, corresponding to dipoles oriented perpendicular to the c axis, are also assumed to be energetically equivalent to one another and associated with an energy parameter ε^S. It is assumed, in other words, that the energy of the crystal in the absence of external electric

fields is given by the number of those dipoles which are perpendicular to the c axis multiplied by the constant parameter ε^S. If however, an electric field E is applied along the positive c axis, then the crystal energy is decreased by an amount which is equal to the product of E and the electric moment of the crystal along $+c$. Calling μ the dipole moment, it follows that the internal energy of the crystal in the presence of a field E is:

$$U = N_0 \varepsilon^S - (N_+ - N_-)\,\mu E, \qquad \text{(III-25)}$$

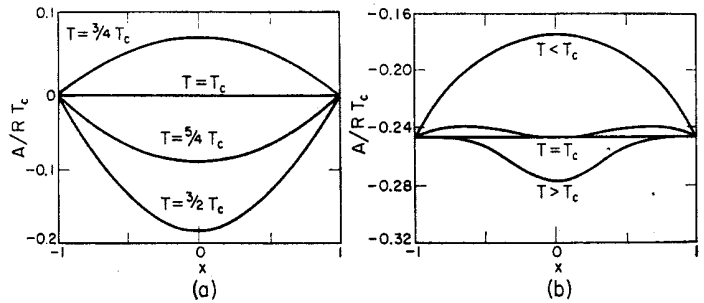

FIG. III-21. Free energy as a function of relative polarization: (a) according to Slater's theory (S 4); (b) according to Yomosa and Nagamiya (Y 1).

where N_0, N_+ and N_- are the numbers of $(H_2PO_4)^-$ dipoles pointing across, up, and down the tetragonal c axis, respectively. ($N_0 + N_+ + N_- = N$, where N is the total number of dipoles.) There are many ways in which a state N_+, N_-, N_0 can be realized, and the problem is to find the number $W(N_+, N_-, N_0)$ of arrangements of the hydrogens which lead to such a state. If we can solve this problem, we can compute the entropy of the system as $S = k \cdot \ln W(N_+, N_-, N_0)$, where k is the Boltzmann constant, and apply the usual thermodynamic formalism to compute the dielectric and thermal properties of the crystal.

Slater finds an expression for the function $W(N_+, N_-, N_0)$ by counting the number of the pertinent hydrogen arrangements with a method that consists of building up the crystal molecule by molecule. He assumes that, at a given step in the process of building up, the crystal already contains a certain number of molecules and that he adds another molecule to the surface. Considering the various ways in which the hydrogens of this new molecule can be arranged, he then finds how the number of arrangements increases on account of the addition of this molecule. He finally arrives at a formula for $W(N_+, N_-, N_0)$. Takagi (T 3) obtained exactly the same formula using a different counting procedure.

When the function W is known the free energy $A(N_+, N_-, N_0) = U - TS$ can be computed. The condition for a minimum of the free energy allows the elimination of N_0 and the expression of the free energy in terms of the variable $x = (N_+ - N_-)/N$. Figure III-21 (a) is a graphical representation of $A(x)$ for the case $E = 0$: $x = \pm 1$ corresponds to the fully polarized state and $x = 0$ to the unpolarized state. The latter is stable for temperatures $T > T_c$, the former occurs for $T < T_c$. At the transition temperature T_c, the crystal goes from the unpolarized to the *fully* polarized state.

Thus, the function W leads directly to the *existence* of a phase change. The Curie temperature T_c is given by the formula:

$$kT_c = \frac{\varepsilon^S}{\ln 2}, \tag{III-26}$$

and is, therefore, directly proportional to the energy parameter ε^S. The theory accounts for the temperature dependence of the dielectric susceptibility in a satisfactory way, leading to the Curie–Weiss law:

$$\frac{\partial P}{\partial E} = \frac{N\mu^2}{k \ln 2} \frac{1}{T - T_c}. \tag{III-27}$$

The entropy difference between the polarized and the unpolarized state is computed to be 0.69 cal/mole °C at the Curie temperature. Above the transition, the theory predicts an additional entropy increase, spread over a wide temperature range, such as to give a total entropy difference of 0.805 cal/mole °C. These entropy changes are in satisfactory agreement with the experimental results (see Table III-1).

The character of the transition predicted by Slater's theory is very remarkable. It is a very unusual type of transition, as every intermediate state between the fully unpolarized and the completely polarized state is just as stable as the initial and the final state. It is similar to the usual transition of the first order insofar as polarization and energy undergo discontinuous changes and there is latent heat. On the other hand, it is similar to a transition of the second order, insofar as the phase change takes place in a homogeneous way and thus every quantity is continuous in time; it could be considered as the limiting case of a second order transition.

Experimentally, as we know, the transition is not sudden, but takes place through a finite temperature range. Slater attributes the observed gradual increase of the spontaneous polarization and the λ-type anomaly of the specific heat to irregular distribution of stresses within the crystal, caused by the spontaneous strain, which give rise to different transition temperatures for different domains.

In spite of this explanation, some objections have been raised against Slater's theory because of the discrepancy with the experimental data concerning the character of the transition. Since the theory is treating the tetragonally clamped crystal, it is reasonable to ask whether the free crystal could have a second-order transition. Forsbergh (F 2) has shown that this is in fact the case, but only if the relation between strain and polarization is complemented with saturation terms, as in Eq. (III-3).

One may also ask whether Slater's result is due to the counting procedure followed for the derivation of the function $W(N_+, N_-, N_0)$. This question was answered by Takahashi (T 1), who approached the same model of Slater in a different way. He formally replaced the hydrogen bonds with "arrows" and studied how many configurations of arrow "chains" are possible, within the crystal, for a certain number of positive and negative chains to exist. In this terminology, Slater's second assumption (ii) is equivalent to saying that, at each

PO_4 group, there are two in-going and two out-going "arrows". Takahashi computed the partition function rigorously for all possible chain configurations and arrived at exactly the same result as Slater, i.e. a discontinuous transition for which, at $T = T_c$, the states involving any arbitrary ratio between the numbers of positive and negative chains are equally stable.

One then could think of changing the character of Slater's transition by modifying the theory in such a way as to include the deformation of the crystal, due to piezoelectric interaction, thus accounting also for the anomalous piezoelectric effect. This approach is due to Yomosa and Nagamiya (Y 1). If the crystal is strained with the shear x_y, the PO_4 groups will change their orientation and the configurational energy of the crystal will also change. This fact is taken into account by assuming that the energy difference between a $(H_2PO_4)^-$ group polarized along $+c$ or $-c$ and a group polarized perpendicular to c is a linear function of the strain. Calling ε_+ the energy of a positive group, ε_- that of a negative group, it is postulated that:

$$\varepsilon_+ = -\varepsilon^S - \beta x_y$$

$$\varepsilon_- = -\varepsilon^S + \beta x_y$$

The fact that, in the strained crystal, the four orientations of a $(H_2PO_4)^-$ group polarized perpendicular to the c axis are no longer equivalent is neglected. Slater's formula (III-25) becomes, under these assumptions:

$$U = N_+ \varepsilon_+ + N_- \varepsilon_- - (N_+ - N_-)\mu E + \tfrac{1}{2} a N x_y^2 - \tfrac{1}{2} k E^2 - f x_y E \tag{III-28}$$

where the fourth term represents that part of the elastic energy which is independent of the hydrogen-bond configurations, the fifth term is the energy due to the polarization induced by an external field (independently of the hydrogen bond configuration), and the last term represents the interaction energy between the polarization induced piezoelectrically by the strain x_y (not involving the hydrogen bonds), and the field E.

Combining this U function with Slater's W function, a free energy function is found which allows the discussion of the dielectric, piezoelectric and elastic properties of the crystal. This theory yields very satisfactory results in that it predicts a difference of 3.7 °C between the transition temperature of the free crystal and that of the clamped crystal, in agreement with the experimental results (see Section 2), and it predicts a spontaneous deformation of the free crystal, below the transition, in the form of a shear $x_y = 26'$, also in excellent agreement with the experimental data (see Section 3). The theory predicts, in addition, an anomaly of the elastic compliance s_{66}^E at the transition temperature; the thermal behavior of s_{66}^E is quantitatively in good agreement with the measurements. The character of the transition is changed, with respect to that given by Slater's theory, insofar as there is a range in temperature in which the states with $x = 0$ and $x = \pm 1$ coexist. Figure III-21 (b) shows the free energy as a function of x as obtained from this theory. The transition is now typically of the first order. Thus, although the modifications suggested by Yomosa and Nagamiya lead to considerable improvements of the original Slater's theory, the discontinuous character of the transition is still in disagreement with the experimental results.

This discrepancy, however, can be avoided by only slightly relieving the infinitely tight interrelations of hydrogen positions expressed by Slater's assumptions (i) and (ii) (see p. 96). Relief of the first assumption was undertaken by Shirane and Oguchi (S 5), who allowed a small probability that two or no hydrogens can temporarily reside on any one of the bonds. Relief of the second assumption was studied by Takagi (T 2), who allowed a small probability for the existence of (H_3PO_4) or $(HPO_4)^{2-}$ groups. In both cases, an energy parameter ε_i is assigned to what, in each case, can be considered a lattice imperfection, and the effect of a change in the ratio $\varepsilon_i/\varepsilon^S$ from zero to infinity on the character of the transition is studied. It is found that Slater's step function is rounded off with decreasing values of $\varepsilon_i/\varepsilon^S$, and satisfactory agreement with the experimental data is reached when $\varepsilon_i/\varepsilon^S$ ranges from 5 to 10. This result is in keeping with the expectation that the probability of occurrence of these lattice imperfections must be rather low. However, there is no direct proof that the value of this ratio is appropriate.

A different approach to Slater's model has recently been made by Grindlay and ter Haar (G 1). A positive or negative dipole moment is assigned to a hydrogen bond according to whether the proton occupies one or the other of the two possible equilibrium positions along the bond. Each bond interacts with three other bonds on each of the two PO_4 groups it connects. If only nearest-neighbor interactions are considered, the problem is essentially one of the Ising type. Treatment of this problem with the Bethe method (B 15) under consideration of Slater's assumption (ii) yields results which are fully equivalent to those of Slater's calculations. The treatment is thereafter extended along the path indicated by Takagi (T 2), with the difference that not only configurations such as H_3PO_4 and $(HPO_4)^{2-}$ are allowed, but also configurations such as $(H_4PO_4)^+$ and $(PO_4)^{3-}$. The energy parameters associated with these four configurations are chosen to be ε_i, ε_i, $2\varepsilon_i$ and $2\varepsilon_i$, respectively, while the energy associated with the configuration $(H_2PO_4)^-$ is normalized to zero, as in Slater's theory. The result of the theory of Grindlay and ter Haar shows that the order of the transition depends on the ratio $\varepsilon_i/\varepsilon^S$ where ε^S is Slater's energy parameter. If $\varepsilon_i/\varepsilon^S > \frac{3}{2}$, the transition is of the first order; if $\varepsilon_i/\varepsilon^S < \frac{3}{2}$, the transition is of the second order. The authors do not report the value of the ratio $\varepsilon_i/\varepsilon^S$ which yields quantitative agreement with the experimental data, but this value must necessarily be smaller than the value of 10 obtained by Takagi. The discrepancy may arise from the fact that the latter assumed the probability for the configurations (H_4PO_4) and $(PO_4)^{3-}$ to be zero. This approximation, however, may be closer to the truth than the rather high probability assumed for these configurations by Grindlay and ter Haar.

In conclusion, the objections raised against Slater's theory because of the character of the transition that it predicts should not be considered very serious. The theory can be made to predict a second-order transition, as we have seen, upon consideration of very reasonable points, such as the existence of a small concentration of lattice imperfections.

A more serious objection to Slater's theory is rather the fact that it cannot explain the large isotope effect, i.e. the almost doubling of the transition temperature in going from KH_2PO_4 to KD_2PO_4. Since in Slater's theory the transition temperature is given by Eq. (III-26) this means that, at the transition temperature, $\varepsilon^S = KT_c \ln 2$, and there is no apparent reason why the energy difference ε^S between dipoles pointing along and perpendicular to c should nearly be doubled when H is replaced by D. It is true that the deuterated crystal shows an increase in the lattice constant along the a axis by 0.25% with respect to the hydrogenated compound (U 2), but it cannot be said whether or not this is sufficient to explain the doubling of the value of ε^S.

An attempt at explaining the isotope effect within the framework of Slater's theory has recently been made by Senko (S 8) by introducing into the model the contributions due to dipole–dipole interactions. The new free energy function relates with one another the changes in Curie temperature and in spontaneous polarization caused by deuterium substitution. This improved model accounts rather satisfactorily for the shift in Curie point and for the temperature and field dependence of the dielectric constant, but is rather inaccurate in its predictions of the transition entropy and the temperature dependence of the spontaneous polarization in the vicinity of the Curie temperature.

Theory of Pirenne

Another possibility, due to Pirenne, is to consider the protons as anharmonic oscillators moving in a certain potential well V (interaction between protons and neighboring atoms). The spontaneous polarization is assumed to be entirely due to dipole–dipole interaction. The actual crystal polarization is divided into two parts:

(i) the polarization P_p due to displacements of the protons, which carry an effective charge ne $(n < 1)$; and

(ii) the polarization P_b of the "background" due to all other causes (electronic polarization, displacements of ions other than H). P_b is assumed proportional to P_p.

The dipole–dipole interaction is taken care of by means of a molecular field γP_p. Then, for a polarized state to be in equilibrium, V must be anharmonic and the simplest case is to treat the oscillators quantum-mechanically as particles in a square well potential. Now, when H is replaced by D, every vibrational energy level is lowered by a factor 2, since the mass is doubled, and thus becomes twice more polarizable. The energy E_0 of the first vibration level is found to be $E_0 = 0.683 \times 10^{-2}$ eV. This predicts an absorption band of energy $3E_0$, i.e. in the region 166 cm^{-1} for KH_2PO_4 and 83 cm^{-1} for KD_2PO_4, which is in fair agreement with the infrared data, as pointed out by Pirenne (P 4).

The theory yields a value of $\gamma = 5.97$, which is not too far from the Lorentz value $4\pi/3 = 4.18$, and a value of $n = 0.27$, which does not differ much from the value in water, $n = 0.40$. The agreement between theory and experiment is good as far as the saturation polarizations, the Curie constants and the heat of

transitions of the hydrogenated and the deuterated crystals are observed. The ratio of proton polarization to total polarization, P_p/P, is found to be rather small, 0.206, suggesting that the background polarization is playing an important role.

Concluding, Pirenne's theory is certainly successful in its attempt to explain the isotope effect. It is probable, however, as mentioned by Forsbergh (F 2), that all other possibilities suggested to explain the isotope effect also contribute and co-operate to give the large change observed.

While Pirenne used a single-minimum potential field, Blinc (B 17), more recently, assumes a double-minimum potential in which tunneling of the protons in the hydrogen bonds is allowed. Blinc's theory is essentially a quantum-mechanical treatment of the simple local-field theory developed by Mason and Devonshire (see below). In addition to explaining the infrared and the nuclear magnetic resonance data (see also Section III-7), the theory accounts fairly well for the isotope effects. Its weakness lies mainly in the fact that it does not take into account short-range interactions, which have proven so effective in Slater's model.

Long-range Interactions

Insofar as Pirenne's theory introduces a molecular field proportional to the polarization, to account for the dipolar interaction, this theory can be considered one involving long-range forces, in contrast to Slater's treatment. Two other theories have been proposed for KDP using the long-range interactions, namely the theory of Mason (M 1) and that of Grindlay and ter Haar (G 1).

Mason's theory associates a dipole moment μ to each hydrogen bond. The bond potential is assumed to be symmetrical. The interaction between the dipoles is taken care of by means of an internal field

$$F = E + \frac{4\pi}{3} P_b + \gamma P_d,$$

where P_d is the dipole polarization and P_b the background polarization. The latter is put equal to $\alpha_b F$, where α_b is the polarizability per unit volume due to the background only (without the hydrogens). The quantity α_b can be determined from the temperature-independent part of the dielectric constant:

$$\frac{4\pi}{3} \alpha_b = \frac{\varepsilon_0 - 1}{\varepsilon_0 + 2}.$$

An expression for the *clamped* dielectric constant is obtained:

$$\varepsilon^x = \varepsilon_0 + \frac{C}{T - T_0},$$

where C and T_0 are functions of the number of dipoles per unit volume, the dipole moment μ and the Lorentz factor γ. Comparison with the experimental data leads to the following values of μ and γ:

$$\mu = 0.81 \times 10^{-18} \text{ c.g.s.}; \quad \gamma = 0.567,$$

where μ is independent of temperature. The theory predicts a polarization much larger than that observed. Mason justifies this discrepancy by judging that the experimental values of the spontaneous polarization are too small, owing to the fact that at low temperatures the largest fields applied are not sufficient to reverse all the domains.

Devonshire (D 1) has pointed out that the model involving dipoles with two positions of equilibrium does not fit the case of KDP very well. The potential well responsible for the dipoles is probably one intermediate between the two extreme cases depicted schematically in Fig. I-2.

The theory of Grindlay and ter Haar (G 1) assumes a dipolar hydrogen lattice interpenetrating *ionic* lattices of potassium, phosphorous and oxygen. The long-range interactions are taken into account by the Lorentz internal-field approximation and the ionic parameters of the K, P and O lattices are computed with the method of Born and Huang. The theory leads to a qualitative understanding of the ferroelectric behavior of KDP but includes two serious quantitative inconsistencies. Since the driving fields from the hydrogen lattice on to the potassium and phosphorous sites have the same sign, the theory requires that the displacements of K and P occur in the same direction, in contrast to the results of the structural analyses. In order for these displacements to be in opposite directions, the K and P ions must have effective charges of opposite sign, a fact which is in disagreement with the expected behavior of electropositive ions. Furthermore, the theory cannot account for both the temperature dependent and the temperature independent part of the dielectric constant. The authors (G 1) point out that the failure of the ionic model is in line with the expectation that the ionic content of KDP is rather low.

9. Domains and Effects of Particle Size

Direct evidence for the existence of domains in the ferroelectric phase of KH_2PO_4 was first given by the X-ray investigations of de Quervain (D 2), and of Ubbelohde and Woodward (U 3) and by the optical study of Zwicker and Scherrer (Z 2). Domain patterns were later observed under the polarizing microscope by Mitsui and Furuichi (M 6), but no systematic investigations were carried out, mainly because the low temperatures at which the polar phase appear make such an experimental study quite difficult. It is not difficult, on the other hand, to predict what the domain structure should look like from our knowledge of the low-temperature symmetry and the lattice distortion. Figure III-22 shows a schematic drawing of two equivalent domain configurations which are compatible with the spontaneous strain x_y. Direct observation of these domain patterns should be possible, under favorable conditions, with the polarizing microscope, because the domains with opposite polarization have, in the position depicted in Fig. III-22, slightly different extinction positions. However, no experimental information is available, to date, concerning the details of the domain structure and the dynamic properties of domains in KDP.

Some information about the energy and the thickness of domain walls can be gained indirectly from experiments concerned with the effect of particle size. Such experiments were carried out by Känzig and co-workers (K 2), (K 3), (J 2) and were stimulated by the following argument. Since a rigorous mathematical treatment of a practical case is almost hopeless, the case of an insulated non-conducting spherical crystal, which is forced to be uniformly polarized, was considered. The depolarizing energy of such a single-domain crystal would be:

$$U_E = \tfrac{1}{2}\frac{4\pi}{3} P^2 V$$

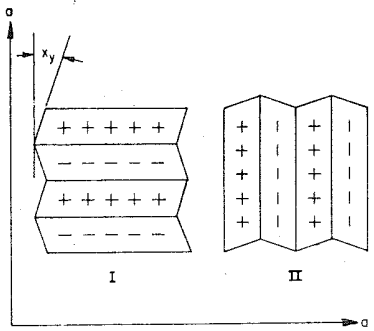

FIG. III-22. Expected domain patterns in KH_2PO_4 (schematic) (according to Känzig (K 4)).

where V is the volume, while the energy of transition,

$$U_Q = \frac{2\pi}{C} T_c P^2 V$$

(see Eq. II-4) is so much smaller than U_E that the hypothesized polarized state cannot occur unless the electrostatic energy is reduced either by conduction or formation of domains. Since conduction is negligible at low-temperatures, the only mechanism left to decrease the depolarizing energy in a *perfect* KH_2PO_4 crystal is that of domain formation. The domain wall energy is a surface energy; if the dimensions of the crystal are decreased, it is reasonable to expect that this surface energy will become important, with respect to the volume energies, below a certain critical size of the crystal. It will then be energetically more favorable to do without the domain walls and the whole crystal will be forced to become a single domain. Then the polarization will be annihilated by the depolarizing field and the crystal will no longer be ferroelectric. It should be noted (K 4) that this effect has no counterpart in ferromagnetic crystals, as the magnetostatic self-energy is always about 10^3 times smaller than the transition energy and thus cannot suppress the spontaneous magnetization.

Experiments were carried out on colloidal particles of KH_2PO_4 imbedded in an insulating medium with an effective dielectric constant of about 5. X-ray and electron diffraction techniques, as well as dielectric measurements were used to detect the ferroelectric transition. The results show that no spontaneous deformation occurs in particles with diameter smaller than 1500 Å. It is concluded from this that particles of this size no longer polarize spontaneously. On the other hand, particles larger than 4000 Å still show the normal ferroelectric behavior of large crystals. As expected, the critical particle size is found to decrease with increasing dielectric constant of the imbedding medium until, when the latter becomes conducting, no critical size exists (particles with diameter of about 500 Å are still found to be ferroelectric in a conducting medium).

The evaluation of these results in terms of wall energy and wall thickness requires the development of a molecular theory of the wall on the basis of a model. Since the treatment of a realistic model is exceedingly difficult, Känzig and Sommerhalder (K 3) considered the simple model of a body-centered cubic lattice occupied by point dipoles pointing along [001] at the absolute zero of temperature. The domain wall was assumed to be parallel to the (100) plane and its energy calculated from the difference between the interaction energies of the state with the wall and the state without the wall, respectively. The dipolar wall energy was found to be $\sigma_{dip} = 0.88\, P^2 a$, where P is the value of the polarization inside the domains and a is the lattice constant. This formula could be used for a crude estimate of the order of magnitude of the wall energy in KH_2PO_4 using the critical particle size determined experimentally. It was concluded that the wall energy is of the order of 40 ergs/cm² and the wall thickness from 2 to 3 unit cells.

Other molecular models for the domain wall in KH_2PO_4 were proposed (B 5), involving both "polarized" walls (where the dipole vectors are rotated by 90° at the time) and "neutral" walls (where the dipole moments are reduced to zero within the wall), but their rigorous mathematical treatment is very difficult.

BIBLIOGRAPHY

(B 1) BUSCH, G. and SCHERRER, P., *Naturwiss.* **23**, 737 (1935).
(B 2) BUSCH, G., *Helv. Phys. Acta* **11**, 269 (1938).
(B 3) BAUMGARTNER, H., *Helv. Phys. Acta* **24**, 326 (1951).
(B 4) BAUMGARTNER, H., *Helv. Phys. Acta* **23**, 651 (1950).
(B 5) BARKLA, H. M. and FINLAYSON, D. M., *Phil. Mag.* **44**, 109 (1953).
(B 6) BANTLE, W., *Helv. Phys. Acta* **15**, 373 (1942).
(B 7) BANTLE, W. and CAFLISH, C., *Helv. Phys. Acta* **16**, 235 (1943).
(B 8) BERGMANN, L., *Der Ultraschall*, Hirzel Verlag, Zürich (1954).
(B 9) BACON, G. E., *Neutron Diffraction*, Clarendon Press, Oxford (1955).
(B 10) BACON, G. E. and PEASE, R. S., *Proc. Roy. Soc.* (*London*) **A 220**, 397 (1953).
(B 11) BACON, G. E. and PEASE, R. S., *Proc. Roy. Soc.* (*London*) **A 230**, 359 (1955).
(B 12) BJORKSTAM, J. L. and UEHLING, E. A., *Phys. Rev.* **114**, 961 (1959).
(B 13) BAUMGARTNER, H., JONA, F. and KÄNZIG, W., *Ergeb. exakt. Naturwiss.* **23**, 235 (1950).

(B 14) BLINC, R. and HADZI, D., *Molec. Phys.* **1**, 391 (1958).
(B 15) BETHE, H., *Proc. Roy. Soc.* (*London*) **A 150**, 552 (1935).
(B 16) BECK, M. and GRÄNICHER, H., *Helv. Phys. Acta* **23**, 522 (1950).
(B 17) BLINC, R., *J. Phys. Chem. Solids* **13**, 204 (1960).
(C 1) CADY, W. G., *Piezoelectricity*, McGraw-Hill, New York (1946).
(D 1) DEVONSHIRE, A. F., *Theory of Ferroelectrics*, *Phil. Mag.* Suppl. **3**, 85 (1954).
(D 2) DE QUERVAIN, M., *Helv. Phys. Acta* **17**, 509 (1944).
(D 3) DANNER, H. R. and PEPINSKY, R., *Phys. Rev.* **99**, 1215 (1955).
(E 1) ESS, H., Thesis, Eidg. Techn. Hochschule, Zürich (1946). Unpublished.
(F 1) FRAZER, B. C. and PEPINSKY, R., *Acta Cryst.* **6**, 273 (1953).
(F 2) FORSBERGH, P. W., JR., *Piezoelectricity, Electrostriction and Ferroelectricity*, *Handbuch der Physik*, vol. 17, pp. 264–392, Springer-Verlag, Berlin (1956).
(G 1) GRINDLAY, J. and TER HAAR, D., *Proc. Roy. Soc.* (*London*) **A 250**, 266 (1959).
(J 1) JONA, F., *Helv. Phys. Acta* **23**, 795 (1950).
(J 2) JACCARD, C., KÄNZIG W. and PETER, M., *Helv. Phys. Acta* **26**, 521 (1953).
(K 1) KETELAAR, J. A. A., *Acta Cryst.* **7**, 691 (1954).
(K 2) KÄNZIG, W., *Phys. Rev.* **87**, 385 (1952).
(K 3) KÄNZIG, W. and SOMMERHALDER, R., *Helv. Phys. Acta* **26**, 603 (1953).
(K 4) KÄNZIG, W., *Ferroelectrics and Antiferroelectrics*, *Solid State Physics*, vol. 4, pp. 1–197, Academic Press, New York (1957).
(L 1) LEVY, H. A., PETERSON, S. W. and SIMONSEN, S. H., *Phys. Rev.* **93**, 1120 (1954).
(L 2) LANDSBERG, G. S. and BARYSHANSKAYA, F. S., *Doklady Akad. Nauk S.S.S.R.* **61**, 1027 (1948).
(L 3) LORD, R. C. and MERRIFIELD, R. E., *J. Chem. Phys.* **21**, 166 (1953).
(M 1) MASON, W. P., *Piezoelectric Crystals and their Application to Ultrasonics*, Van Nostrand, New York (1950).
(M 2) MASON, W. P., *Phys. Rev.* **69**, 173 (1946).
(M 3) MATTHIAS, B. T., *Phys. Rev.* **85**, 723 (1952).
(M 4) MEGAW, H. D., *Ferroelectricity in Crystals*, Methuen, London (1957).
(M 5) MURPHY, G. M., WEINER, G. and OBERLY, J. J., *J. Chem. Phys.* **22**, 1322 (1954).
(M 6) MITSUI, T. and FURUICHI, J., *Phys. Rev.* **90**, 193 (1953).
(M 7) MATTHIAS, B. and MERZ, W., *Helv. Phys. Acta* **19**, 227 (1946).
(N 1) NEWMAN, R., *J. Chem. Phys.* **18**, 669 (1950).
(O 1) OBERLY, J. J. and WEINER, G., *J. Chem. Phys.* **20**, 740 (1952).
(P 1) POCKELS, F., *Lehrbuch der Kristalloptik*, Teubner, Leipzig (1906).
(P 2) PETERSON, S. W., LEVY, A. H. and SIMONSEN, S. H., *J. Chem. Phys.* **21**, 2084 (1953).
(P 3) PELAH, I., LEFKOWITZ, I., KLEY, W. and TUNKELO, E., *Phys. Rev. Letters* **2**, 94 (1959).
(P 4) PIRENNE, J., *Helv. Phys. Acta* **22**, 479 (1949).
(P 5) PAULING, L., *J. Am. Chem. Soc.* **57**, 2680 (1935).
(P 6) PIRENNE, J., *Physica* **15**, 1019 (1949).
(R 1) RUNDLE, R. E. and PARASOL, M., *J. Chem. Phys.* **20**, 1487 (1952).
(S 1) STEPHENSON, C. C. and HOOLEY, J. G., *J. Am. Chem. Soc.* **66**, 1397 (1944).
(S 2) STEPHENSON, C. C., CORBELLA, J. M. and RUSSELL, L. A., *J. Chem. Phys.* **21**, 1110 (1953).
(S 3) SEIDL, F., *Tschermak's mineral. u. petrog. Mitt.* **1**, 432 (1950).
(S 4) SLATER, J. C., *J. Chem. Phys.* **9**, 16 (1941).
(S 5) SHIRANE, G. and OGUCHI, T., *J. Phys. Soc. Japan* **4**, 172 (1949).
(S 6) STEPHENSON, C. C. and ZETTLEMOYER, A. C., *J. Am. Chem. Soc.* **66**, 1402 (1944).
(S 7) SHIRANE, G., JONA, F. and R. PEPINSKY, *Proc. I.R.E.* **43**, 1738 (1955).
(S 8) SENKO, M., *Phys. Rev.* **121**, 1599 (1961).

(T 1) TAKAHASHI, H., *Proc. Phys. Math. Soc. Japan* **23**, 1069 (1941).
(T 2) TAKAGI, Y., *J. Phys. Soc. Japan* **3**, 271 (1948).
(T 3) TAKAGI, Y., *Proc. Phys. Math. Soc. Japan* **23**, 44 (1941).
(U 1) UBBELOHDE, A. R. and WOODWARD, I., *Proc. Roy. Soc.* (*London*) **A 188**, 358 (1947).
(U 2) UBBELOHDE, A. R. and WOODWARD, I., *Proc. Roy. Soc.* (*London*) **179**, 399 (1942).
(U 3) UBBELOHDE, A. R. and WOODWARD, I., *Nature* **156**, 20 (1945).
(U 4) UNTERLEITNER, F., OKAYA, Y., VEDAM, K. and PEPINSKY, R., *Abstracts Annual Meeting Am. Cryst. Assoc.*, Ithaca, New York, July (1959).
(V 1) VON ARX, A. and BANTLE, W., *Helv. Phys. Acta* **17**, 298 (1944).
(V 2) VON ARX, A. and BANTLE, W., *Helv. Phys. Acta* **16**, 211 (1943).
(Y 1) YOMOSA, S. and NAGAMIYA, T., *Progr. Theoret. Phys.* **4**, 263 (1949).
(W 1) WALKER, A. C., *J. Franklin Inst.* **250**, 481 (1950).
(W 2) WEST, J., *Z. Krist.* **74**, 306 (1930).
(Z 1) ZWICKER, B., *Helv. Phys. Acta* **19**, 523 (1946).
(Z 2) ZWICKER, B., and SCHERRER, P., *Helv. Phys. Acta* **17**, 346 (1944).